Metabolomics

FUNCTIONAL GENOMICS AND METABOLOMICS REVEAL THE TOXICOLOGICAL EFFECTS OF CADMIUM IN Mus musculus MICE

--Manuscript Draft--

Manuscript Number:	MEBO-D-14-00302R3
Full Title:	FUNCTIONAL GENOMICS AND METABOLOMICS REVEAL THE TOXICOLOGICAL EFFECTS OF CADMIUM IN Mus musculus MICE
Article Type:	Original Article
Keywords:	biological response; qRT-PCR; absolute transcription profiles; 2DE-DIGE proteomics; Metabolomics; Mus musculus; cadmium exposure; direct infusion mass spectrometry
Corresponding Author:	Jose-Luis Gomez-Ariza, Ph.D. University of Huelva HUELVA, SPAIN
Corresponding Author Secondary Information:	
Corresponding Author's Institution:	University of Huelva
Corresponding Author's Secondary Institution:	
First Author:	Miguel Angel Garcia-Sevillano, Ms.
First Author Secondary Information:	
Order of Authors:	Miguel Angel Garcia-Sevillano, Ms.
	Nieves Abril, Dr
	Ricardo Fernández-Cisnal, Dr
	Tamara Garcia-Barrera, Dr
	Carmen Pueyo, Prof
	Juan Lopez-Barea, Prof
	Jose-Luis Gomez-Ariza, Ph.D.
Order of Authors Secondary Information:	
Funding Information:	
Abstract:	Cadmium (Cd) is an environmental pollutant that accumulates in the organisms causing serious health problems. Over the past decades, "omics" studies have been conducted trying to elucidate changes in the genome, the transcriptome or the proteome after Cd exposure. Metabolomics is relatively new to the "omics" revolution, but has shown enormous potential for investigating biological systems or their perturbations. When metabolomic data are interpreted in combination with genomic, transcriptomic and proteomic results, in the co-called systems biology approach, a holistic knowledge of the organism/process under investigation can be achieved. In this work, transcriptional and proteomic analysis (functional genomics) were combined with metabolomic workflow to evaluate the biological responses caused in Mus musculus mice by Cd (subcutaneous injection for 10 consecutive days). Animals showed high Cd levels in liver and plasma, drastic lipid peroxidation in liver, increased transcription of hepatic genes involved in oxidative stress, metal transport, immune response and lipid metabolism and moderate decreases of DNA repair genes mRNAs. 2DE-DIGE proteomics confirmed changes of hepatic proteins related to stress and immune responses, or involved in energy metabolism, suggesting a metabolic switch in the liver from oxidative phosphorylation to aerobic glycolysis, that was confirmed by metabolomics analysis, via DIMS and GC-MS. This metabolic alteration is particularly important for highly proliferating cells, like tumor cells, which require a continuous supply of precursors for the synthesis of lipids, proteins and nucleic acids. The metabolic changes observed in mouse liver by metabolomics and the oxidative stress

	detected via functional genomics could be in the base of Cd hepatocarcinogenicity.

FUNCTIONAL GENOMICS AND METABOLOMICS REVEAL THE TOXICOLOGICAL EFFECTS OF CADMIUM IN *Mus musculus* MICE

M.A. García-Sevillano[a,b,c,§], N. Abril[d,e,§], R. Fernández-Cisnal[d,e], T. García-Barrera[a,b,c], C. Pueyo[d,e], J. López-Barea[d,e], J.L. Gómez-Ariza[a,b,c,] *

MEBO-D-14-00302R1

Correspondign autor: **J.L. Gómez-Ariza**

- A conflict of interest statement has been included

FUNCTIONAL GENOMICS AND METABOLOMICS REVEAL THE TOXICOLOGICAL EFFECTS OF CADMIUM IN *Mus musculus* MICE

M.A. García-Sevillano[a,b,c,§], N. Abril[d,e,§], R. Fernández-Cisnal[d,e], T. García-Barrera[a,b,c], C. Pueyo[d,e], J. López-Barea[d,e], J.L. Gómez-Ariza[a,b,c,] *

[a]Department of Chemistry and Materials Sciences, Faculty of Experimental Science, [e]Agrifood Campus of International Excellence (ceiA3-UHU) and [c]Research Center of Health and Environment (CYSMA), University of Huelva, Campus de El Carmen, 21007-Huelva, SPAIN.

[d]Department of Biochemistry and Molecular Biology and [e]Agrifood Campus of International Excellence (ceiA3-UCO), University of Córdoba, Severo Ochoa Building, Rabanales Campus, 14071-Córdoba, SPAIN.

[§]Both authors contributed equally to this work and should be considered first authors.

***Corresponding Author**: José Luis Gómez Ariza. Tel.: +34 959 219968, fax: +34 959 219942, e-mail address: ariza@uhu.es

Abbreviated title: Toxicological effects of cadmium in mice

Acknowledgements. This project received grants CTM2012-38720-C03-01 and CTM2012-38720-C03-02 from the Ministerio de Economia y Competitividad-Spain; BIO1675, P12-FQM-00442 and P09-FQM-04659 from the Consejería de Innovación, Andalusian government. M.A. García-Sevillano thanks to Ministerio de Educación for a predoctoral grant.

Abstract

Cadmium (Cd) is an environmental pollutant that accumulates in the organisms causing serious health problems. Over the past decades, "*omics*" studies have been conducted trying to elucidate changes in the genome, the transcriptome or the proteome after Cd exposure. Metabolomics is relatively new to the "*omics*" revolution, but has shown enormous potential for investigating biological systems or their perturbations. When metabolomic data are interpreted in combination with genomic, transcriptomic and proteomic results, in the co-called systems biology approach, a holistic knowledge of the organism/process under investigation can be achieved. In this work, transcriptional and proteomic analysis (functional genomics) were combined with metabolomic workflow to evaluate the biological responses caused in *Mus musculus* mice by Cd (subcutaneous injection for 10 consecutive days). Animals showed high Cd levels in liver and plasma, drastic lipid peroxidation in liver, increased transcription of hepatic genes involved in oxidative stress, metal transport, immune response and lipid metabolism and moderate decreases of DNA repair genes mRNAs. 2DE-DIGE proteomics confirmed changes of hepatic proteins related to stress and immune responses, or involved in energy metabolism, suggesting a metabolic switch in the liver from oxidative phosphorylation to aerobic glycolysis, that was confirmed by metabolomics analysis, via DIMS and GC-MS. This metabolic alteration is particularly important for highly proliferating cells, like tumor cells, which require a continuous supply of precursors for the synthesis of lipids, proteins and nucleic acids. The metabolic changes observed in mouse liver by metabolomics and the oxidative stress detected via functional genomics could be in the base of Cd hepatocarcinogenicity.

Keywords: Biological response, qRT-PCR; absolute transcription profiles; 2DE-DIGE proteomics, metabolomics, *Mus musculus*, cadmium exposure, direct infusion mass spectrometry

1. Introduction

Cadmium has become one of the most important environmental pollutants in the world due to its wide application in a variety of industrial processes. Cd accumulates mainly in the liver and kidney and both organs are critical targets for acute Cd toxicity (Goyer and Clarkson, 2001; Jihen el et al., 2010; Nordberg, 2009). Several reports indicate that Cd toxicity involves depletion of reduced glutathione (GSH), inhibition of antioxidant enzymes and of energy metabolism and enhanced production of reactive oxygen species (ROS) (Zhai et al., 2013). Thus, increased lipid peroxidation and oxidative DNA damage, inflammatory processes, apoptosis and necrosis have been described among the mechanisms of Cd-induced liver injury (Afolabi et al., 2012; Asara et al., 2013; Brzoska and Rogalska, 2013; Brzoska et al., 2011; Filipič, 2012; Jihen el et al., 2010; Jurczuk et al., 2003; Jurczuk et al., 2004; Koyu et al., 2006; Matovic et al., 2011; Moniuszko-Jakoniuk et al., 2005; Murugavel and Pari, 2007b; Rana, 2008; Rani et al., 2014; Satarug et al., 2010; Templeton and Liu, 2010).

In recent years, the massive advances in the knowledge of genes and genomes (genomics) prompted the development of several novel "*omics*" very useful to reveal the biological responses of organisms to toxic metal exposure and to understand the toxicity mechanisms of contaminants (Garcia-Sevillano et al., 2014b). Fundamental biological processes can now be studied by applying to one biological sample the full range of "*omics*" technologies (Morrison et al., 2006). Genomics applies methods of Molecular Biology and Bioinformatics to sequence, assemble and analyze the structure and function of genomes (the complete set of DNA within a single cell of an organism). In contrast, Functional Genomics deals with the analysis of gene expression (Transcriptomics) and the comprehensive analysis of proteins/metalloproteins (Proteomics/Metalloproteomics) (Gonzalez-Fernandez et al., 2008). More recently, Metabolomics, the complete study of metabolites involved in different metabolic processes, has become an emerging field in analytical biochemistry and can be regarded as the end point of "*omics*" cascade (Dettmer and Hammock, 2004). Furthermore, since changes in the metabolome are the ultimate response of an organism to genetic alterations or environmental influences, the metabolome is most predictive of phenotype (Fiehn, 2002; Weckwerth, 2010). Thus, the comprehensive and quantitative study of transcripts, proteins and metabolites is an attractive tool for either diagnosing pathology or studying the effects of toxicants on phenotype in the organism under investigation.

Although Cd has been related with several pathologies, the mechanisms underlying Cd toxicity are not yet fully elucidated. We have used here a combination of transcriptomics, proteomics and metabolomics methodologies to obtain a holistic view of the molecular pathways altered by Cd exposure over 10 consecutive days aimed to determine the biochemical consequences for mice. Effects in the hepatic transcriptional profile were measured by absolute quantitative reverse transcription-polymerase chain reaction (qRT-PCR) analysis, combined to 2-DE difference gel electrophoresis (DIGE) to evaluate the perturbations in the liver proteome. These results were complemented with metabolomics data obtained by applying the metabolomic workflow based in the use of molecular mass spectrometry to liver and plasma of *Mus musculus* mice.

2 Materials and methods

2.1 Animal handling

Mus musculus (inbred BALB/c strain) mice were obtained from Charles River Laboratory (Spain). A total of 32 male mice of 7 weeks were allowed to acclimate for 5 days with free access to food and water under controlled conditions (25-30ºC, 12 h light-dark photoperiod) prior to the exposure. For the experiment, mice were distributed into four groups, two being exposed to Cd(II) (as $CdCl_2$) by subcutaneous injection (100 µl) of a solution of 0.1 mg Cd per kg of body weight per day and the other two groups used as control and injected with 100 µL of 0.9% NaCl in ultrapure water. A control and a Cd-treated group of mice were sacrificed at the 6^{th} day of the experience and the other two groups at the 10^{th} day. After being individually anesthetized by isoflurane inhalation, mice were sacrificed by cervical dislocation and exsanguinated by cardiac puncture, dissected using a ceramic scalpel and their organs transferred rapidly to dry ice. Individual organs were weighted in Eppendorf vials, rinsed in 0.9% NaCl solution, frozen in liquid nitrogen and stored at -80 ºC. Individual livers were ground by cryogenic homogenization. Three pools were prepared per experimental condition (control or Cd-treated groups, after 6d and 10d) by mixing equal amounts of homogenized hepatic tissue or plasma from 2-3 mice per pool; each pool represented a biological replicate. The experimental design is pictured in Online Supporting Information Figure 1. Mice were handled according to the norms stipulated by the European Community. The investigation was approved by the Ethics Committees of Córdoba and Huelva Universities (Spain).

2.2 Determination of cadmium concentration in liver and plasma

A SPEX SamplePrep cryogenic homogenizer (Freezer/Mills 6770) was used for solid tissue disruption. Cd concentration was determined in mouse liver and plasma after 6 and 10 days of treatment. Samples (0.100 g) were exactly weighed in 5-ml PTFE microwave vessels and mixed with 500µL of a HNO_3/H_2O_2 mixture (4:1 v/v) (Ultra Trace analytical grade, Fisher Scientific, Leicestershire, UK). After 10 min, the vessels were closed and introduced into a MARS microwave oven (CEM Matthews, NC, USA). The mineralization was carried out at 400 W, starting at room temperature, ramping to 160ºC in 15 min, and holding for 20 min at 160ºC. Then the solutions were made up to 2 g with ultrapure water and trace metals were analyzed with an Agilent 7500ce inductively coupled plasma mass spectrometer

(Agilent Technologies, Tokyo, Japan) equipped with an octopole collision/reaction cell. The element Rh was added as internal standard (1µg /l). All analyses were made using three replicates and previously published operating conditions (Garcia-Sevillano et al., 2012).

2.3 Measurement of lipid peroxidation in liver

Lipid peroxidation was measured as thiobarbituric acid reactive substances (TBARS). Three pools were prepared per each experimental condition (Cd-treated and control groups, after 6d and 10d) by mixing equal amounts of homogenized hepatic tissue ~~or plasma~~ of 2-3 mice per pool; each pool represented biological replicates. Of each sample, 100 mg were disrupted in 300 µL of 10 mM Tris-HCl, pH 7.5, containing 1 mM EDTA, 1 mM GSH and 1 mM PMSF and the lipid peroxides in the homogenate were determined by the Buege and Aust (1978) method with some modifications. Briefly, 2-10 µL of lysates were mixed with 125 µL of 0.5% (w/v) butylated hydroxytoluene in methanol, 50 µL of 0.66 N H_2SO_4 and 37.5 µL of 0.4 M Na_2WO_4, and the total volume was adjusted to 1 mL with water. Samples were vortexed and centrifugated (5000 g, 5 min, at room T) and the supernatant mixed with 250 µL of 1% thiobarbituric acid (w/v in NaOH 0.1M). Mixtures were heated at 95 ºC for 1 hour, cooled to room T in an ice bath, and their fluorescence was determined (Ex/Em 515/550 nm, 15 nm slit width) in a LS 50B fluorescence spectrometer (Perkin Elmer). The TBARS concentrations in each sample were determined from a standard curve generated from 1,1,3,3-tetraethoxypropane and expressed as nmol of MDA formed per 100 mg of tissue. All determinations were carried out in triplicate.

2.4 Absolute quantification of mRNA levels by qRT-PCR

Primer design. Primers directed against mouse *Sod1*, *MT1* and *A170* genes were designed with the Oligo 7.58 software (Molecular Biology Insights) with identical characteristics (Pueyo et al., 2002) to other primers used in this work and previously described (Abril et al., 2014; Fuentes-Almagro et al., 2012; Jurado et al., 2007; Prieto-Alamo et al., 2003). All primers are given in Online Supporting Information Table 1.

RNA sample preparation. Total RNA from individual livers was isolated with the RNeasy Mini Kit (Qiagen) and the resulting RNA was further treated with DNase I (QIAGEN RNase-Free DNase Set) to remove residual DNA. The samples were then cleaned up with the same RNeasy Mini Kit, using the RNA

Clean Up protocol and denatured by heating at 65ºC for 10 min. RNA integrity was determined by microcapillary electrophoresis with the Agilent 2100 Bioanalyzer, and RNA concentrations were accurately measured using the Hellma TrayCell system (Hellma Analytics). Genomic DNA contamination was tested by PCR amplifications of RNA samples without prior cDNA synthesis. Three pools per experimental condition (Cd-treated and control groups after 6 and 10d) were prepared by mixing equal amounts of total RNA of 2-3 mice and used for cDNA synthesis.

qRT-PCR. The absolute quantification of mRNA levels was carried out as described (Jurado et al., 2007). cDNA was generated from 2 µg of pooled RNA and real-time PCR reactions were performed in quadruplicate with 50 ng/well of cDNA. An absolute calibration curve was constructed with 10^2 to 10^9 molecules per well of an *in vitro* synthesized RNA (Jurado et al., 2007; Prieto-Alamo et al., 2003). The number of transcript molecules was calculated from the linear regression of the calibration curve (Jurado et al., 2007; Prieto-Alamo et al., 2003). The reliability of an absolute quantification depends on identical amplification efficiencies for both the target and the calibrator. Our primers were designed to amplify all amplicons with optimal (~100%) efficiencies and high linearity ($r > 0.99$) in the range of 20 to 2×10^5 pg of total RNA input.

2.5 DIGE experiment

Protein extraction. One pool was prepared per each of the two Cd-exposed groups (6 and 10d) by mixing equal amounts of ground liver from the 8 mice included in each group; equal amounts of liver from all control mice were pooled in one unique control (Online Supporting Information Figure 1). From each tissue pool (control, 6d- and 10d-Cd exposed) 100 mg were disrupted in 300 µL of extraction buffer (20 mM Tris-HCl, pH 7.6, containing 0.5 M sucrose, 0.15M KCl, 20 mM DTT, 1 mM PMSF, 6 µM leupeptin and P2714 Sigma Protease Inhibitor after manufacturer´s instructions). Cell debris was cleared by centrifugation (14000 *g*, 10 min, 4ºC) and the supernatants were treated with benzonase (500 U/ml) and ultracentrifuged (105000 *g*, 60 min). These extracts were precipitated by using a 2D-Clean-up kit (GE-Healthcare) after manufacturer's instructions, resuspended in 8 M urea containing 30 mM Tris-HCl and 4% w/v CHAPS and adjusted to pH 8.5. Protein concentration was determined using 2D-Quant Kit (GE Healthcare).

Fluorescent labelling of proteins and 2-DE electrophoresis. Protein samples were labeled using Cy3 and Cy5 dyes (CyDye™ DIGE Fluor minimal, GE Healthcare) after manufacturer's instructions. All samples in the experiment were mixed, labeled with Cy2 dye for use as internal standard (IS) for normalization. Equal amounts (50 μg) of one Cy3 and one Cy5 labeled samples from different experimental conditions and the Cy2-labeled IS were combined and separated on a single 2DE gel (Cy dyes were swapped to compensate for dye differences). Total volume was adjusted to 50 µL, mixed 1:1 with isoelectrofocusing (IEF) rehydration buffer (8 M urea, 4% w/v CHAPS, 130 mM DTT, 2% w/v IPG buffer pH 3-10) and incubated for 30 min to obtain complete denaturation of proteins. All steps were carried out at 4ºC.

Immobilized pH gradient (IPG) strips (pH 4–7, 24 cm) (GE Healthcare) were rehydrated overnight at 20ºC with 390 µl of DeStreack rehydration solution (GE Healthcare) containing 2% w/v of IPG buffer pH 4-7. Then, denatured proteins were cup-loaded in the IPG strips at approximately 1 cm from the cathode. After 6 h active (50 V) rehydration, IEF was carried out (20°C, 50 µA/strip) in a Protean IEF apparatus (Bio-Rad) at 500, 1000, 2000, 4000, 6000 and 8000 V (each 90 min) and 8000 V (until reaching 57 000 Vh). The strips were then soaked 20 min in equilibration mix (50 mM Tris–HCl, pH 8.8, 6 M urea, 30% w/v glycerol, 2% w/v SDS, and bromophenol blue traces) containing 65 mM DTT, drained and again soaked 20 min in this mix containing 0.35 M iodoacetamide. For the second dimension, DryStrips were loaded on top of 12.5% w/v SDS-PAGE gels and separated at 20 °C in a BioRad Protean Plus Dodeca Cell at 2.5 W per gel (10 min) and 3 Wper gel (approx.12 h).

The separated proteins labeled with Cy3, Cy5 and Cy2 dyes were detected in gels using a Typhoon scanner (GE Healthcare). The Cy3- and Cy5-labeled proteins migrating to each 2D spot were quantified based on the corresponding fluorescence intensities and their molar ratios were calculated using the DeCyder 6.5 software (GE Healthcare). Each set of three images from a single gel was first processed using the Differential In-gel Analysis module for automatic spot detection, spot volume quantification and volume ratio normalization of the different samples loaded in the same gel. Then, the Biological Variation Analysis module was used to automatically match the spots among different gels and to identify those showing statistically significant differences between the samples. Statistical analysis (ANOVA) was performed on all spots that exhibited $\geq \pm 1.5$-fold change ($p \leq 0.02$) in protein content.

2.5 In gel digestion and mass spectrometry (MS) analysis

A total of 48 spots corresponding to differentially expressed proteins were selected for identification. Preparative gels were loaded with 300 µg of the IS sample to facilitate matching; protein separation was obtained in the same conditions described above for the DIGE gels. After 2-DE, proteins were stained with Sypro Ruby® (BioRad) according to the manufacturer's instructions, and the selected spots were excised using an Investigator™ProPic station (Genomic Solutions). Spots were destained, dehydrated, and dried. Proteolytic digestion was carried out with 20 µl trypsin (12.5 ng/µl trypsin in 25 mM ammonium bicarbonate) at 25ºC for 10 min followed by 3 x 5 min treatment in a microwave oven (200W). The digestion was stopped by adding 10 ml of 0.5% v/v trifluoroacetic acid (TFA). The resulting peptides were purified in a Pro PrepII station (Genomic Solutions) with a C18 microcolumn (ZipTip, Millipore), eluting with matrix solution (5 mg/ml alpha-Cyano-4-hydroxycinnamic acid in 70% acetonitrile and 0.1% TFA). Samples were directly spotted onto an Opti-TOF® MALDI plate (AB SCIEX) using the Investigator™ ProMS apparatus (Genomic Solutions) and analyzed using an AB SCIEX 4800 MALDI TOF/TOF apparatus, operated in the positive reflection delayed extraction mode. Spectra were internally calibrated using the m/z ratios of the peptides derived from auto-digestion of porcine trypsin (MH 842.509, MH 2211.104). The m/z was measured to a precision of 720 ppm. The MS/MS fragmentation spectra of the most intense 12 m/z fragments were found for each sample. The spectra obtained in the MALDI TOF/TOF analysis, with a signal/noise threshold ≥10, were adjusted to a baseline, deisotoped, and the values of the mono-isotope ions of each peptide were detected.

Molecular masses of the tryptic peptide profiles were used to search in the IPI_Mouse database (http://www.ebi.ac.uk/IPI/IPIhelp.html) with GPS Explorer software v2.0 (Applied Biosystems) and automated database search, using the Mascot Search Engine (Matrix Science). Their masses were compared to the theoretical peptide masses of all available proteins and predicted proteins from DNA sequences. Unmatched peptides were not considered in the analysis. All peptide fragments obtained for each digest were submitted to a search made by combining Peptide Mass Fingerprinting (PMF) and the results from MS/MS fragmentations. Search parameters for the program were as follows: maximum allowed error of peptide mass 100 ppm; cysteine as S-carbamidomethyl-derivative, oxidation of methionine, formation of pyroglutamic acid, and acetylation of the N-terminal extreme allowed.

2.6 Metabolomic workflow

2.6.1 Sample preparation for metabolomics study by mass spectrometry.

All solvents used in sample preparation for the metabolomic study of liver and plasma were of optima LC/MS grade. Methanol, acetonitrile and chloroform were from Fisher Scientific (Leicestershire, UK), while ammonium acetate and formic acid were from Sigma-Aldrich (Steinheim, Germany). Sample preparation of individual livers for metabolomic analysis based on direct infusion to mass spectrometry (DIMS) was carried out in two-steps. 1) *Polar metabolites* were extracted by adding 200 µL of a methanol/acetonitrile mixture (2:1, v/v) to 50 mg tissue in an Eppendorf tube followed by vigorous vortex shaking for 5 min. Then, the cells were disrupted using a pellet mixer (2 min) at 4ºC, and the sample was centrifuged for 10 min at 4000 *g* and 4°C. The supernatant was carefully collected and transferred to another Eppendorf tube. The pellet was re-homogenized as above with 100 µL of methanol/acetonitrile mixture (2:1, v/v), centrifuged as described above and the pellet was kept for further treatment. Both supernatants were combined and stored to -80ºC for analysis. 2) *Lipophilic metabolites* were extracted from the pellet with 200 µL of a chloroform/methanol mixture (2:1, v/v), using a pellet mixer (2 min), and centrifuged at the same conditions described above. The resulting supernatant was stored to -80ºC for analysis.

For DI-ESI(±)-QTOF-MS of blood plasma samples, proteins were removed by adding 400 µL of a methanol/acetonitrile mixture (2:1, v/v) to 100 µL plasma in an Eppendorf tube followed by vigorous vortex shaking for 5 min at room T and centrifugation for 10 min at 4000 *g* and 4 °C. The supernatant was carefully collected avoiding the precipitated proteins, transferred to another Eppendorf tube and the resulting supernatant was taken to dryness under N_2 stream for storage at -80ºC until analysis. To extract lipophilic metabolites, the pellet was homogenized with 200 µL of a chloroform/methanol mixture (2:1, v/v), using a pellet mixer (2 min), and centrifuged for 10 min at 10000 *g* and 4 °C. The resulting supernatant was taken to dryness under N_2 stream and stored at -80ºC for analysis. The polar extracts were reconstituted to 100 µL of a methanol/acetonitrile mixture (2:1, v/v) and the lipophilic extracts were reconstituted to 100 µL of a chloroform/methanol mixture (2:1, v/v) before the analysis by ESI-MS.

For data acquisitions from positive ionization, 0.1 % (v/v) formic acid was added to polar extract and 50 mM of ammonium acetate to lipophilic extract. In the case of negative ionization intact extracts were directly infused to the mass spectrometer.

2.6.2 Analysis of sample extracts by direct infusion-mass spectrometry

Metabolomic experiments of liver and plasma extracts from Cd-exposed mice were performed by DIMS in a QSTAR XL Hybrid system mass spectrometer (Applied Biosystems, Foster City, CA, USA) using an electrospray ionization source (ESI). The parameters for triple quadrupole-time of flight (QqQ-TOF) analyzer were optimized to obtain the higher sensitivity with minimal fragmentation of molecular ions, both in positive and negative ion modes. To acquire MS/MS spectra, N_2 was used as collision gas. Gas chromatography-mass spectrometry (GC-MS) analysis was also applied to mice plasma, as previously described (Garcia-Sevillano et al., 2013). Derivatizing agents, methoxylamine hydrochloride and N-methyl-N-(trimethylsilyl) trifluoroacetamide containing 1% trimethylchlorosilane, were obtained from Sigma-Aldrich.

2.6.3 Analysis of samples by gas chromatography-mass spectrometry

Sample preparation for GC-MS analysis was carried out as a previously published (Garcia-Sevillano et al., 2014a). Separation was performed in a Trace GC ULTRA gas chromatograph coupled to a ITQ900 ion trap mass spectrometer detector, both from Thermo Fisher Scientific, using a Factor Four capillary column VF-5MS 30m×0.25mm ID, with 0.25 µm of film thickness (Varian).

The injector temperature was kept at 280ºC, and He was used as carrier gas at 1 mL/min constant flow rate. For optimal separation, column T was initially maintained at 60ºC for 10 min, and then increased from 60 to 140ºC at a rate of 7 ºC/min and held for 4 min. Then, column T was increased to 180 ºC at 5º C/min and maintained for 6 min. Finally, the T was increased to 320ºC at 5 ºC/min, and held for 2 min. For MS detection, ionization was carried out by electronic impact (EI) with 70 eV voltage, using full scan mode in the m/z range 35–650, with an ion source T of 200ºC. For the analysis, 1 µl of sample was injected in splitless mode. The identification of endogenous metabolites was based on comparison with the corresponding standards according to their retention times and mass spectra characteristics; complementarily, search on NIST Mass Spectral Library (NIST 02) was used.

2.6.4 Data analysis

Markerview™ software (Applied Biosystems) was used to filter the MS results. Statistical data analysis (partial least squares discriminant analysis, PLS-DA) were performed by the SIMCA-P™ statistical software package (v 11.5, UMetrics AB, Umeå, Sweden). PLS-DA is a partial least squares regression of a set Y of binary variables describing the categories of a categorical variable on a set X of predictor variables. It is a compromise between the usual discriminant analysis and a discriminant analysis on the significant principal components of the predictor variables (Perez-Enciso and Tenenhaus, 2003). Data were processed to find differences between mice groups submitted to different exposure time, and to trace the metabolites altered by Cd for later identification by their molecular mass and fragments in

MS/MS experiments. In addition, altered metabolites were characterized using different DIMS-based metabolomics databases, such as Human Metabolome Database (http://www.hmdb.ca), METLIN (http://metlin.scripps.edu) and Mass Bank (http://www.massbank.jp). In GC-MS analysis, metabolite identification was performed using the NIST Mass Spectral Library (NIST 02).

3 Results and discussion

3.1 Determination of cadmium in liver and plasma

The analysis of Cd concentrations in tissue samples revealed a dose-related increase in Cd levels. Male *Mus musculus* mice were daily injected subcutaneously with 0.1 mg Cd per kg of body weight during a total period of 10 days. Data in Online Supporting Information Table 2 shows that Cd accumulation was a gradual process in liver and resulted in >50-fold higher Cd level in the liver of 10d-treated mice compared to the control group, with a >20-fold rise in Cd concentration after 6 days. In plasma a cumulative Cd concentration was found in treated mice, raising from a >12-fold after 6d to >16-fold after 10d, compared to the control group.

3.2 Measurement of lipid peroxidation in liver

Cadmium does not generate free radicals directly, but has been proposed to replace Fe and Cu in various cytoplasmic and membrane proteins. Hence, Cd accumulation in tissues increases the amount of free or chelated Cu and Fe ions participating in oxidative stress via Fenton reactions (Valko et al., 2005). The so generated reactive oxygen species (ROS) cause lipid peroxidation, protein oxidation and DNA damage to the cellular constituents (Fang et al., 2010).

Fig. 1 shows that Cd treatment induced in mice a strong and statistically significant increase of the hepatic MDA levels, a subproduct of lipid peroxidation, according to previous reports (Valko et al., 2005). This MDA increase parallels Cd accumulation in liver and both parameters correlated positively (78.5%) indicating that, irrespectively of the mechanism, Cd caused an intense oxidative stress in the hepatic tissue.

3.3 Transcriptional profile in mouse following cadmium exposure

Both Cd and ROS influence signal transduction processes via the modulation of transcription factors which lead to the transcriptional activation of different genes (Habeebu et al., 2000; Jara-Biedma et al., 2013). Exposure to Cd triggers a cellular antioxidant response via transcriptional regulators, such as the nuclear factor (erythroid-derived 2)-like 2 (Nrf2). Classical Nrf2 target genes are involved in antioxidant defense, including glutathione *S*-transferases, subunits of glutamate–cysteine ligase, heme oxygenase, glutathione peroxidases, peroxiredoxins, and metallothioneins (MT) among others (Kensler et al., 2007; Wu et al., 2012).

Here we have examined in mouse liver the transcriptional responses to Cd exposure, focusing on 14 genes involved in oxidative stress response, metal transport, DNA repair, heat shock response, lipid metabolism and immune response. We worked with three mini-pools prepared by mixing equal amounts of total RNA of 2-3 mice per experimental condition (control and Cd-treated after 6 and 10 days). Since many factors, including animal sacrifice, may contribute to interindividual variability in gene expression, even working with genetically identical mice, we first quantitated by real-time PCR the transcript molecules of three genes, *A170, Mogat1* and *Gpx1* in liver samples of each mouse (8) included in the 6d-control group (Online Supporting Information Table 3). Replicate reactions generated highly reproducible results with SDs <10% of the mean values (<1% of threshold cycle data). Interindividual variations was in the same range, demonstrating that the studied genes have a stable expression in these samples. From these results, we assumed that the study would not be exposed to misinterpretation by using sample pools.

The real-time PCR analysis allowed to accurately assessing the basal expression levels of a selected set of genes in the mice livers, summarized in Figure 2. Genes from low (< 1 mRNA copy/pg of total RNA in the case of *Mogat1*) to high basal expression levels (> 10^3 mRNA copies/pg of total RNA in the case of Gpx1) were determined in a highly quantitative manner. Cd exposure altered the transcript levels of each of the 14 studied genes, chosen as representatives of different stress response pathways, as indicated below.

Stress response

The first set of genes code for the main members of the antioxidant network. SODs dismutate superoxide into O_2 and H_2O_2, subsequently detoxified to H_2O by catalase (CAT) or by members of the glutathione peroxidase (GPX) or peroxiredoxin (PRDX) families (Han et al., 2008). Heme oxygenase 1 (HMO1) disrupts heme, a potent prooxidant and proinflammatory agent, and generates biologically active products such as CO with an important antiinflammatory effect (Jozkowicz et al., 2007). A170, mouse counterpart of the human sequestosome 1 (SQSTM1) or p62, links polyubiquitinated protein aggregates to the autophagic machinery, facilitating their clearance (Bjorkoy et al., 2005). P62/SQSTM1/A170 is a broad negative regulator of cytokine expression that controls the inflammatory response (Kim and Ozato, 2009).

The levels of all these hepatic antioxidant genes rised in a time-dependent manner after Cd exposure, with a significantly higher expression over the control group. Except Gpx1, with a maximum after 6d Cd-treatment, all genes kept rising until 10d exposure. Increases of 2–3 fold over control were found for these 6 genes. Most studies using RT-PCRare are semiquantitative (fold-change) and assume that reference genes are stably expressed, or that any possible changes are balanced. Such assumption biases the interpretation of results, and usually leads to overestimate the role of rare transcripts in the studied process. The absolute expression profiles reported in Figure 2 are not normalized and, thus, do not assume that a reference is steadily expressed. The relevance of data reported here is highlighted when comparing the increments in transcript molecules with the conventional fold variations. Thus, although a 2.32-fold increase in Gpx1 transcripts might look similar to the 2.38-fold rise of Hmo1, the actual scenario is that Gpx1, highly abundant mRNA in liver, exhibited much higher increase in copy number (from ~500 molecules/pg in 6d-control mice to ~1100 molecules/pg in 6d-Cd treated mice) than Hmo1, low abundant mRNA, rising from ~1.4 molecules/pg in 6d-control mice to ~3.3 molecules/pg in 6d-Cd treated mice.

Detoxification of Cd in hepatic cells depends mainly on the induction of metallothioneins (MT), small metal-binding proteins in which 25–30% of all amino acids are cysteine. Cd binds to the thiol groups of MT and is then released by hepatocytes and transported to the kidney in blood plasma. Cd and oxidative stress are particularly strong inducers of MT genes in liver, as reflected in the transcript levels of Mt1 shown in Fig.2. Compared to controls, the livers of Cd-exposed mice showed an impressive and time-dependent increase of Mt-1 mRNA molecules. We have previously reported that Cd exposure also induce MT expression at the protein level, by coupling HPLC with ICP-MS and ESI-MS which permitted us to identify Cd complexes with MT isoforms induced in *Mus musculus* (Jara-Biedma et al., 2013).

Immune response

Cadmium is an immunotoxic that causes disorders in the humoral and cellular immune responses (Afolabi et al., 2012). The first phase of hepatic damage starts by Cd binding to sulfhydryl groups of GSH and proteins, and a second phase is initiated by activation of Kupffer cells, which release proinflammatory cytokines and chemokines (Wu et al., 2012), although the molecular basis for Cd stimulated cytokine expression is unknown. Though Cd specifically induces the transcription of several classes of genes, including those involved in immunity and inflammation, the intermediate events between Cd exposure and induction of cytokine gene expression are not fully defined and may involve numerous pathways (Marth et al., 2001). We found here that Cd caused a strong and sustained rise in the transcript levels of *Pla2g1B* gene reaching 100-fold after 10d treatment (Fig.2). The inflammatory events evoked by pancreatic phospholipase A2, the product of *Pla2g1B,* are thought to be primarily associated with the induction of IL-6 and TNFα from blood monocytes at the transcriptional level (Jo et al., 2004). Hence, *Pla2g1B* induction in liver by Cd might be one of the intermediate events resulting in the induction of cytokine gene expression. Cadmium can also interact with surface structures, inducing the synthesis of immunoglobulins (Igs) (Marth et al., 2001), key humoral components of acquired immunity. A >3-fold increase in the transcripts of Igh gene encoding the Ig heavy chains was observed in the liver of Cd-exposed mice after 10 days (Fig.2), in agreement with the increased IgG and IgM mRNAs described in Cd treated cells (Marth et al., 2001).

DNA repair

DNA damage in Cd-exposed mammalian cells derives from the induction of DNA lesions but also from inactivation of several DNA repair enzymes. BER (base excision repair), key to repair ROS-induced oxidative DNA damage is affected by Cd exposure (Hegde et al., 2008). The mammalian AP-endonuclease, APE1 plays a central role in the BER pathway repairing by DNA glycosylases the apurinic/apyrimidinic (AP) sites generated spontaneously or after excision of oxidized and alkylated bases. The 8-oxoguanine DNA glycosylase 1 (OGG1) repairs 8-oxo-7,8-dihydroguanine, the most frequently formed oxidative DNA base lesion (Hamann et al., 2012). Cadmium extensively decreses the OGG activity in cells and the AP-endonuclease activity from cell extracts or purified APE1 protein (Bravard et al., 2010). Some reports attributed OGG1 and APE1 decrease to diminished transcription of Ogg1 and Ape1 genes, but data are contradictory (Bravard et al., 2010; Hamann et al., 2012; Zhou et al., 2013). Here we confirm that Cd caused a modest decrease in *Ogg1* and *Ape1* transcript molecules, and hence, translational modifications should be the cause of OGG1 and APE1 inhibition described by others (Bravard et al., 2010; Hamann et al., 2012; McNeill et al., 2004).

Lipid metabolism

Though intensively studied in aquatic organisms (i.e., (Fang and Miller, 2012; Lu et al., 2012; Wang and Gallagher, 2013)), there is limited information about the effect of Cd on lipid metabolism in mouse liver. Larregle (Larregle et al., 2008) reported that Cd exposure in rats increased the contents of free fatty acids (FFA), triacylglycerols (TAG) and total cholesterol in liver. The high TAG level in Cd-treated rats was attributed to an increased TAG synthesis. The amounts of mRNA (Fig 2) of two genes, *Mogat1* (~8-fold increase) and *Pla2g1B* (~100-fold increase), suggest that also in the liver of our Cd-treated mice might be higher FFA and TAG levels.

Mogat1 codes for monoacylglycerol acyltransferase-1 active in one of two convergent pathways for TAG biosynthesis, and *Mogat1* up-regulation has been described in mouse models of hepatic steatosis (Cortés et al., 2009; Kang et al., 2011), a major consequence of heavy metal exposure (Garcia-Sevillano et al., 2014c). The *Pla2g1B* induction by Cd (see above) might contribute to the elevate levels of FFA, since PLA2G1B releases fatty acids from dietary phospholipids. The increase in free cholesterol previously observed in the liver of Cd exposed rats (Afolabi et al., 2012; Larregle et al., 2008; Murugavel and Pari, 2007a) has been attributed to enhanced expression of cholesterogenic enzymes including 3-hydroxy-3-methylglutaryl-CoA reductase (HMGCR) and the repression of some cholesterol catabolic pathways. Data in Fig. 2 shown a clear induction at the transcriptional level of *Hmgcr* and *Idi* (isopentenyl-diphosphate delta isomerase 1), two enzymes involved in cholesterol biosynthesis. In fact, *Hmgcr* catalyzes the rate-limiting step in this biosynthetic pathway. The induction of *Hmgcr* might be consequence of *Pla2g1B* induction by Cd and the associated production of IL-6 and TNFα (Murugavel and Pari, 2007b).

The transcriptional analysis reported here draws a global panorama in which Cd caused a strong oxidation of hepatic cells in mice that could not be avoided by the Cd-scavenging action of MT1. The oxidative situation generated affected the lipid metabolism and raised the inflammation response, each being both a cause and effect of the other. Lipids are the main component of cell membranes, and hence alteration of lipid metabolism by Cd might results in alterations in this complex structure.

3.4 Proteomic analysis by DIGE

For the transcriptional study referred above, we selected a group of genes according to the prior knowledge of alterations associated to Cd exposure. Thus, the subsequent results give a directed biological contextualization of their gene signature. An alternative and potentially complementary approach to address this problem is the use of proteomics to assess differences in protein expression profiles. Since the proteome is the protein complement to the genome, proteomic approaches should greatly facilitate the characterization and identification of protein-related changes in mouse liver following Cd administration.

2DE-DIGE analyses were performed in protein extracts from livers of male *Mus musculus* mice daily injected a fixed amount of 0.1 mg Cd/kg of body weight. The livers of mice in each experimental group (6- and 10-days of treatment) were pooled and their proteins extracted. A unique control pool was prepared by mixing equal amounts of homogenized liver from the two control groups. Combinations were made to compare in the same gel each problem pool with any other, labeled with Cy3 in some cases and with Cy5 in others, to correct the dye effect (dye-swapping). The Cy2 dye was used to label the internal standard, obtained by mixing an equal amount of all samples, allowing a significant quantitative comparison of proteomic variations. Six gels were run to achieve a statistically significant measure of the differences in protein expression between the control and the Cd-treated samples. A representative 2D-DIGE gel is depicted in Online Supporting Information Fig. 1. Raw data are accessible from the authors upon request.

The subsequent data analysis detected over 2700 protein spots on each CyDye-labeled gel, in the 4–7 pH range and 14–70 kDa Mr. All protein spots were then quantified, normalized and inter-gel matched. No significant differences were found in mouse liver samples after 2d of Cd exposure, and hence, comparisons were focused on 6d and 10d treated samples. To test for significant differences in protein expression between problem and control samples, the data were filtered using the average volume ratios of ±1.5-fold differences and a t-test p value ≤0.02 and assigned to a spot of interest. Forty-eight spots satisfied these requirements and were excised from the gel for subsequent in-gel digestion and MS analysis for protein identification. Data were submitted to MASCOT database search resulting in the identification of 16 proteins (Table 1). Several proteins were found in different isoforms or with different post-translational modifications and then detected in multiple spots, including aldehyde dehydrogenase family 1 member L1 (ALDH1L1, spots 704 and 750) and fibrinogen gamma chain (FGG, spots 1484 and 1500). Among proteins showing significant correlations with Cd concentrations in exposed mice, 5 proteins (7 spots) were up-regulated and 9 down-regulated. The fold-change variation of these 16 spots after 10 consecutive days of Cd-exposure are indicated in Fig. 3.

The identified proteins were submitted to a functional annotation analysis with the Ingenuity Pathway Analysis (IPA®, QIAGEN Redwood City) to unravel their primary role in cell metabolism.

They were grouped into three categories, involved in the *stress response* (7 proteins, 8 spots), the *immune response* (4 proteins, 5 spots) and *energy homeostasis* (3 proteins).

Stress response

Although we initially expected that most proteins deregulated by Cd treatment would have antioxidant functions, other types of stress response genes were predominant (Table 1 and Fig. 3). Most of these proteins have no obvious antioxidant function, except possibly ALDH1L1 (spots 704 and 750) and OAT (ornithine aminotransferase, spot 2597). ALDH1L1 is highly expressed in the liver under Nrf2 control (Abdullah et al., 2012) that regulates the antioxidant response. It is involved in apoptosis (Hoeferlin et al., 2013) and in the detoxification of the intermediate-chain-length aldehydes, byproducts of lipid peroxidation (Yadav and Ramana, 2013). OAT, mainly found in the liver, is a pyridoxal-phosphate dependent mitochondrial matrix aminotransferase involved in the metabolism of ornithine, shown to be up-regulated during ROS-related apoptosis (Lei et al., 2008). Both proteins were up-regulated in the liver of Cd-treated *M.musculus* mice, corroborating the strong oxidative stress detected (Fig. 1) and suggested by the transcriptional data (Fig. 2).

Three protein spots (1091, 1061 and 991), identified as heat shock proteins (GRP78, HSPA9 and TRAP1, respectively) had lower expression in the livers of Cd-treated mice. Cadmium induces the expression of Glucose-regulated protein 78 (GRP78) in certain cell types but not in hepatocytes (Liu et al., 2006). Fig. 3 show that GRP78 was down-regulated in the liver of 10d Cd-exposed mice. This molecular chaperone is a central regulator of the endoplasmic reticulum (ER) function due to its roles in protein folding. GRP78 induction is an important pro-survival component of the unfolded protein response (Li and Lee, 2006) but it is also a restraint to Nrf2 activation (Chang et al., 2012). Down-regulating GRP78 in Cd-treated mice livers might activate the transcription of genes under Nrf2 control, encoding for phase II/III enzymes and the defense against oxidative stress (Chang et al., 2012). Similarly, HSP9 (Heat shock 70kDa protein 9/mortalin/ GRP75) and TRAP1 (tumor necrosis factor receptor associated protein 1) are mitochondrial heat shock cytoprotective proteins related to drug resistance and protection from apoptosis by buffering reactive oxygen species (ROS)-mediated oxidative stress. Their down-regulation in Cd-treated mice probably impaired mitochondrial functions but also enhanced the apoptosis and avoided mitotic defects and chromosome instability in Cd affected hepatic cells (Agorreta et al., 2014; Ma et al., 2006), where DNA repair is compromised as indicated by the decrease in the transcript levels of Ogg1 and Ape1 genes (Fig.2).

PDIA6 (spot 1499), also known as P5 or TXNDC7, is one of more than 20 protein disulfide isomerases (PDIs) in the eukaryotic ER. It is an active oxidoreductase with similar properties to other PDIs, yet it does not seem to be involved directly in protein folding (Eletto et al., 2014). By contrast, PDIA6, limits the duration of the unfolded protein response (UPR) and it has been reported that PDIA6-deficient cells hyperrespond to ER stress, resulting in exaggerated up-regulation of UPR target genes and increased apoptosis (Eletto et al., 2014). All these results suggest that Cd exposure affects genes involved in cell division and particularly mechanisms that are responsible to cell cycle arrest. Our results could indicate that Cd exposure represses hepatocyte division. This hypothesis is further supported by the fact that Cd exposure was also associated with the down-regulation of the heterogeneous nuclear ribonucleoprotein K (hnRNPK, spot 1343), involved in cell signaling and gene expression, cooperating with p53 in transcriptional activation of cell-cycle arrest genes after DNA damage (Pelisch et al., 2012). The loss of hnRNPK in Cd-treated hepatic cells might deregulate genes involved in DNA repair, cell proliferation and apoptosis (Yang et al., 2013). Cadmium has been recently reported (Galano et al., 2014) to interfere with protein folding, leading to accumulation of misfolded proteins and ER stress by decreasing chaperone levels.

Immune response

Increasing evidence demonstrates that Cd induces inflammation (i.e., (Marth et al., 2001)), but its mechanisms remain obscure. Our study showed that Cd exposure was positively associated with the systemic inflammation marker fibrinogen, a soluble glycoprotein synthesized by hepatocytes composed by three distinct polypeptides called Aα, Bβ and γ. Fibrinogen is considered an acute-phase reactant and increased fibrinogen content in the blood is considered an indicator for a proinflammatory state (Davalos and Akassoglou, 2012). Three spots up-regulated by Cd in mouse liver were identified as FGB (spot 1298) and FGG (spots 1484 and 1500). Alpha 1-antitrypsin (AAT) is the archetypal member of the serine proteinase inhibitor (SERPIN) gene family. AAT is an acute-phase reactant and the plasma concentration increases three- to four-fold during the inflammatory response. It has been reported that Cd lowers ATT content and depresses the trypsin inhibitory capacity, an effect not shared with any other divalent ions, Pb, Hg, Ni, Fe, and Zn. Other reports show that in mice Cd inhibits chymotrypsin activity *in vivo*

(Shimada et al., 2000). We found here a down-regulation of ATT isoform Serpin 1c (spot 1562) and chymotrypsinogen B (CTRB, spot 2248) in the liver of Cd-treated mice. Serine proteases inhibition has been described as an integral part of the apoptotic response (King et al., 2004) which agrees with down-regulation of GRP78 and other heat shock proteins. These results would also sustain the pro-inflammatory situation evoked by the increased levels of *Pla2g1B* and *Igh* transcripts (Fig. 2), which probably results in the induction of cytokine gene expression and of the synthesis of immunoglobulins described for Cd (Jo et al., 2004; Marth et al., 2001).

Energy metabolism

Though the energy metabolism class is composed by only 3 proteins, they show great metabolic alterations in the liver of Cd-treated mice. Mitochondrial ATPase synthase b subunit (spot 1532) was down-regulated, suggesting a decreased ATP supply by oxidative phosphorylation during Cd exposure. Phosphoglucomutase (PGM1, spot 1216) that catalyze reversible reactions required for glycolysis and gluconeogenesis was up-regulated in the Cd-treated mice livers, probably to meet the enhanced energy demand caused by Cd and to compensate the decrease of oxidative phosphorylation. Finally, down-regulation of $\Delta(3,5)$-$\Delta(2,4)$-dienoyl-CoA isomerase (ECH), an auxiliary enzyme of unsaturated fatty acid β-oxidation might be related to the dysregulation of lipid metabolism described for Cd toxicity.

3.5 Metabolomic analysis by mass spectrometry

For a better understanding of metabolic disorders caused by Cd exposure, we carried out a metabolomic study in the livers of Cd-exposed mice, in parallel to the transcriptional and proteomic analysis. Considering the highly distinct and diverse features of information obtained at the levels of metabolite, mRNA and protein, the combination of these three approaches should provide a highly comprehensive view on the effects of Cd toxicity.

A partial least squares discriminant analysis (PLS-DA) was performed to discriminate between the groups of mice differentially exposed to Cd, assessing the intensities of the signals in the polar and lipophilic extracts from mice plasma and liver, combining the positive and negative ionization mode of acquisition (Fig. 4). The models built with polar and lipophilic metabolites allow a good classification of samples in the different groups, which are shown by the respective scores plots. The *Variable Influence on the Projection* (VIP) parameter was used to identify the variables responsible for this separation. VIP is a weighted sum of squares of the PLS-DA weight that indicates the importance of the variable to the whole model. Thus, it is possible to select variables with the most significant contribution in discriminating between metabonomic profiles corresponding to exposed groups against controls. Only metabolites with VIP > 1.5 have been considered good biomarkers of Cd exposure. The values of R^2Y (cum) and Q^2 (cum) of the combined model are 0.90-0.95 and 0.80-0.90, respectively, indicating that a combination of datasets between groups provides the best classification and prediction. The complementarity of using both ionization modes for polar and lipophilic metabolites is remarkable (see Table 2). In this sense, some metabolites are ionizable using positive and negative mode of acquisition, such as lysophosphatidylcholines, glucose and glutamate, and others are altered in both extracts, such as phosphatidylcholines (Table 2). As a complementary approach, GC-MS was applied also to confirm and quantify altered metabolites established by DIMS and others that are not possible to ionize by ESI. For this purpose, three derivatizing reagents were used for plasma samples to obtain as much metabolic information as possible. Metabolic profiles of mice plasma samples after 6d and 10d of Cd-exposure were obtained by GC-MS.

Table 2 shows a Cd-induced metabolic deregulation, especially of lipids and glucose metabolism. The livers of Cd treated mice had increased levels of triglycerides (TGs), diglycerides (DGs), free fatty acids (10-18C of different unsaturation degree) and lyso-phosphatidylcholines (LPCs), and higher content of choline, phosphocholine, creatinine, glutamine and lactic acid. In contrast, Cd-exposure decreased the levels of glucose, taurine, glutamate, phenylalanine, creatine, citrate and phosphatidylcholines (PCs) in plasma/liver. Via GC-MS we assessed the plasma content of glucose, isoleucine, glutamate, α-ketoglutarate, phenylalanine, isocitrate and citrate and the increase of lactic acid, glutamine and cholesterol levels, to establish the statistical significance of the variation (Table 2). The metabolic changes observed during Cd exposure can be related to perturbations in different metabolic pathways, as follows:

Carbohydrate metabolism

The levels of energy metabolism intermediates, including glucose and three tricarboxylic acid (TCA) cycle members, citrate, isocitrate and α-ketoglutarate, decrease in mouse liver/plasma under Cd exposure (Table 2). TCA is a core pathway for sugar, lipid, and amino acid metabolism. Besides being responsible for production of reducing cofactors (NADH and $CoQH_2$) which fuel the mitochondrial electron transport chain (ETC) to generate ATP, TCA also provides precursors for biosynthesis of lipid, proteins and nucleic acids (Desideri et al., 2014). It was proposed that Cd exerts its toxic effect mainly blocking the ETC by impairing the electron flow through the cytochrome *bc1* complex (Cannino et al., 2009) (Adiele et al., 2012). Since TCA regulation depends primarily on NAD^+ and ADP availability, ETC blocking would reduce the TCA activity and the concentration of its components. A second, non-excluding, mechanism that can explain the lower levels of some TCA cycle components is the oxidation by Cd of aconitase, isocitrate dehydrogenase (IDH) and α-ketoglutarate dehydrogenase (α-KGDH) enzymes (Kil et al., 2006) (Tretter and Adam-Vizi, 2005), impairing the conversion of citrate in succinyl-CoA; actually these enzymes are very sensitive to oxidative stress. Instead, citrate would be exported to the cytosol and cleaved by ATP-citrate lyase (ACLY) to acetyl-CoA and oxaloacetate. While acetyl-CoA is essential to sustain *de novo* FFA synthesis, oxaloacetate can fuel the Krebs cycle if glutamate is available and feeds the cycle via α-KG (Tretter and Adam-Vizi, 2005) and some generation of NAD(P)H in the Krebs cycle is maintained despite of aconitase being blocked. This segment of the Krebs cycle has been suggested to function in the absence of glucose, such as that we observed in Cd treated mice, and may also explain the low levels of citrate and glutamate (Table 2). It is known that mitochondrial respiratory dysfunction results in a switch from oxidative phosphorylation to aerobic glycolysis (the Warburg effect) (Fig. 5). Increased glycolysis confers growth advantages by diverting glucose to generate NADPH and acetyl-CoA and activates factors involved in fatty acid biosynthesis (Tong et al., 2011). Under this metabolic shift, most of the pyruvate generated from glucose (>90%) is converted to lactate by lactate dehydrogenase to recover the NAD^+ needed to maintain glycolysis, produce ATP and assure cell survival (Desideri et al., 2014). Metabolites quantification (Table 2) suggested the onset of aerobic glycolysis in the liver and plasma of Cd-treated mice. Two other evidences from the proteomic study support this idea. First, the up-regulation of PGM1 (Fig. 3) to assure the provision of glucose to the glycolytic pathway. Second, the down-regulation of TRAP1 (Fig. 3) the mitochondrial chaperone that binds to and inhibits succinate dehydrogenase, may alleviate the inhibition of mitochondrial respiration and promote FA oxidation, TCA cycle intermediates, ATP and enhance cell survival. Large amount of evidence points towards this metabolic shift as being particularly important for highly proliferating cells, like tumor cells, which require a continuous supply of precursors for the synthesis of lipids, proteins and nucleic acids (Desideri et al., 2014). From our results, the drastic metabolic changes observed by metabolomics and the extensive oxidative stress detected via functional genomics approaches could also be in the base of cadmium carcinogenicity.

We realize that the changes we observed in the transcripts, proteins and metabolites levels in mice plasma/liver can be influenced by alterations caused by Cd in other tissues. Nephrotoxicity is one of the main adverse effects of cadmium exposure (Rani et al., 2014), and references herein). As a consequence, Cd resulted in inhibition of glucose uptake by kidney and glucosuria (Kothinti et al., 2010), and references herein), which may be in the origin of the hypoglycemia we detected in plasma by metabolomics (Table 2). Growing epidemiological studies have suggested a possible link between Cd exposure and diabetes as Cd induced oxidative stress causes suppression of insulin secretion and apoptosis in pancreatic islet β-cell (Chang et al., 2013). However, our data showed that cadmium-induced hypoglycemia remains in plasm and indicate that the effects of cadmium on the metabolic routes described in the manuscript (genomics, proteomics and metabolomics findings) may be, at least in part, independent of the hormonal action.

Lipid metabolism

Reprogramming of lipid metabolism, in particular fatty acid synthesis, is an important underlying feature of Cd toxicity. Coupled with changes in glycolysis and the TCA cycle is increased expression of genes encoding key enzymes in FA and cholesterol biosynthesis. Data in Table 2 show that Cd exposure resulted in significantly increased FFA, DGA, TGA and total cholesterol contents in liver/plasma. These results fully agree with those in Fig. 2 indicating that the increased mRNA levels of *Mogat1* (~8-fold), *Pla2g1B* (~100-fold), *Hmgcr* (~3-fold) and *Idi1* (~3-fold) paralleled an increase in the corresponding proteins and lead to lipid metabolism dysregulation. Data also corroborate and extend the knowledge of how Cd increase plasma TGA levels, by rising the hepatic synthesis of TAG and not only by decreased lipoprotein lipase activity that leads to an increase in the circulating triglyceride-rich VLDL (Larregle et al., 2008) (Afolabi et al., 2012). Notice that a lipogenic phenotype is considered as a new hallmark of many cancer cells (Dakubo, 2010). (Desideri et al., 2014).

Membrane lipids are particularly sensitive to free radicals due to the presence of polyunsaturated fatty acids, which preferentially undergo lipid peroxidation. The increased levels of choline and phosphocholine detected in liver and plasma (Table 2) after Cd intake may be associated with Cd induced disruption of cell membranes via peroxidation due to the increased oxidative stress. Phosphatidylcholines (PC) are also major components of biological membranes that incorporate choline as a headgroup, and have an important role in both proliferative growth and programmed cell death. As shown in Table 2, Cd diminished PC levels, what probably can be achieved by increasing the levels of PLA2G1B (see Fig. 2 showing increased transcript levels for Pla2g1b gene) that liberate FA and lyso-PC from PC (Ridgway, 2013).

Amino acid metabolism

Alterations of glucose and amino acid levels seem to be a common response to many toxins in several species. Glutamine is the most abundant naturally occurring amino acid in the body whose metabolism is accelerated during the glucose shift to provide substrates for increased lipogenesis and nucleic acid biosynthesis that are critical to the proliferative cell (Dakubo, 2010). Adaptive accelerated glutamine metabolism imposes an increased glutamine intake that is used mainly (66%) to generate lactate and alanine (Dakubo, 2010). Other metabolites increased under Cd exposure were the amino acids aspartate, valine, glycine and serine, all of them considered gluconeogenic. By contrast, the ketogenic amino acids isoleucine and phenylalanine, were decreased in the liver/plasma of Cd treated mice.

Two small metabolites, taurine and creatine, were decreased in the liver/plasma of Cd-treated mice (Table 2). Taurine (2-aminoethanesulfonic acid), a derivative of cysteine, is the most abundant free amino acid in liver with an important antioxidant role (Manna et al., 2009), that might be linked to the oxidative stress promoted by Cd exposure. It is abundantly maintained in the liver by both endogenous biosynthesis and exogenous transport, but is decreased in liver diseases (Miyazaki and Matsuzaki, 2014). Creatine synthesis requires three amino acids: glycine, methionine and arginine. The decreased levels of creatine in Cd-treated mice livers may be originated by the perturbation of transmethylation caused by the increased choline levels (Table 2). Moreover, carnitine is readily degraded to creatinine to be exported to the urea cycle. Elevation of plasma creatinine concentrations (Table 2) might indicate renal damage.

4 Concluding remarks (200 words max.)

Assessment of metal toxicity in mice requires multi-disciplinary tools to integrate many metabolic pathways and biological responses. "*Omics*" technologies are valuable since they provide massive information about biomolecules in cells and organisms under toxic metals effects. We confirm here that successful application of transcriptional analysis (RT-PCR) of a select group of genes, lipid peroxidation assays, proteomic methods (DIGE) and metabolomic workflow (DIMS and GC-MS) for overall evaluation of Cd-induced perturbations in liver and plasma is due to integration of different *omics*. Our integrated results show a critical effect of Cd on the oxidative status, the immune response, the energy metabolism and the lipid metabolism in the liver of Cd treated *Mus musculus* mice for up to 10 days exposure. Data suggest the occurrence of a metabolic switch from oxidative phosphorylation to aerobic glycolysis. This metabolic alteration is particularly important for highly proliferating cells, like tumor cells, which require a continuous supply of precursors for the synthesis of lipids, proteins and nucleic acids. Hence, the metabolic changes observed by metabolomics and the oxidative stress detected via transcriptional analysis and proteomic methods could also be in the base of Cd carcinogenicity.

Conflict of interest

The authors declare no conflict of interest

Compliance with ethical requirements

Animals were handled according to the directive 2010/63/EU stipulated by the European Community, and the study was approved by the Ethics Committees of University of Córdoba and Huelva Universities (Spain).

References

Abdullah, A., N.R. Kitteringham, R.E. Jenkins, C. Goldring, L. Higgins, M. Yamamoto, J. Hayes, and B.K. Park. 2012. Analysis of the role of Nrf2 in the expression of liver proteins in mice using two-dimensional gel-based proteomics. *Pharmacological reports : PR*. 64:680-697.

Abril, N., J. Ruiz-Laguna, M.A. Garcia-Sevillano, A.M. Mata, J.L. Gomez-Ariza, and C. Pueyo. 2014. Heterologous Microarray Analysis of Transcriptome Alterations in Mus spretus Mice Living in an Industrial Settlement. *Environ Sci Technol*. 48:2183-2192.

Adiele, R.C., D. Stevens, and C. Kamunde. 2012. Differential inhibition of electron transport chain enzyme complexes by cadmium and calcium in isolated rainbow trout (Oncorhynchus mykiss) hepatic mitochondria. *Toxicological sciences : an official journal of the Society of Toxicology*. 127:110-119.

Afolabi, O.K., E.B. Oyewo, A.S. Adekunle, O.T. Adedosu, and A.L. Adedeji. 2012. Impaired lipid levels and inflammatory response in rats exposed to cadmium. *EXCLI Journal* 11:677-687.

Agorreta, J., J. Hu, D. Liu, D. Delia, H. Turley, D.J.P. Ferguson, F. Iborra, M.J. Pajares, M. Larrayoz, I. Zudaire, R. Pio, L.M. Montuenga, A.L. Harris, K. Gatter, and F. Pezzella. 2014. TRAP1 Regulates Proliferation, Mitochondrial Function and has Prognostic Significance in NSCLC. *Molecular Cancer Research*.

Asara, Y., J.A. Marchal, E. Carrasco, H. Boulaiz, G. Solinas, P. Bandiera, M.A. Garcia, C. Farace, A. Montella, and R. Madeddu. 2013. Cadmium modifies the cell cycle and apoptotic profiles of human breast cancer cells treated with 5-fluorouracil. *International journal of molecular sciences*. 14:16600-16616.

Bjorkoy, G., T. Lamark, A. Brech, H. Outzen, M. Perander, A. Overvatn, H. Stenmark, and T. Johansen. 2005. p62/SQSTM1 forms protein aggregates degraded by autophagy and has a protective effect on huntingtin-induced cell death. *The Journal of cell biology*. 171:603-614.

Bravard, A., A. Campalans, M. Vacher, B. Gouget, C. Levalois, S. Chevillard, and J.P. Radicella. 2010. Inactivation by oxidation and recruitment into stress granules of hOGG1 but not APE1 in human cells exposed to sub-lethal concentrations of cadmium. *Mutation Research/Fundamental and Molecular Mechanisms of Mutagenesis*. 685:61-69.

Brzoska, M.M., and J. Rogalska. 2013. Protective effect of zinc supplementation against cadmium-induced oxidative stress and the RANK/RANKL/OPG system imbalance in the bone tissue of rats. *Toxicol Appl Pharmacol*. 272:208-220.

Brzoska, M.M., J. Rogalska, and E. Kupraszewicz. 2011. The involvement of oxidative stress in the mechanisms of damaging cadmium action in bone tissue: a study in a rat model of moderate and relatively high human exposure. *Toxicol Appl Pharmacol*. 250:327-335.

Cannino, G., E. Ferruggia, C. Luparello, and A.M. Rinaldi. 2009. Cadmium and mitochondria. *Mitochondrion*. 9:377-384.

Cortés, V.A., D.E. Curtis, S. Sukumaran, X. Shao, V. Parameswara, S. Rashid, A.R. Smith, J. Ren, V. Esser, R.E. Hammer, A.K. Agarwal, J.D. Horton, and A. Garg. 2009. Molecular mechanisms of hepatic steatosis and insulin resistance in the AGPAT2-deficient mouse model of congenital generalized lipodystrophy. *Cell metabolism*. 9:165-176.

Chang, K.-C., C.-C. Hsu, S.-H. Liu, C.-C. Su, C.-C. Yen, M.-J. Lee, K.-L. Chen, T.-J. Ho, D.-Z. Hung, C.-C. Wu, T.-H. Lu, Y.-C. Su, Y.-W. Chen, and C.-F. Huang. 2013. Cadmium Induces Apoptosis in Pancreatic β-Cells through a Mitochondria-Dependent Pathway: The Role of Oxidative Stress-Mediated c-Jun N-Terminal Kinase Activation. *PLoS ONE*. 8:e54374.

Chang, Y.J., Y.P. Huang, Z.L. Li, and C.H. Chen. 2012. GRP78 knockdown enhances apoptosis via the down-regulation of oxidative stress and Akt pathway after epirubicin treatment in colon cancer DLD-1 cells. *PLoS One*. 7:e35123.

Dakubo, G.D. 2010. The Warburg Phenomenon and Other Metabolic Alterations of Cancer Cells. *In* Mitochondrial Genetics and Cancer. Springer-Verlag, Berlin, Heidelberg.

Davalos, D., and K. Akassoglou. 2012. Fibrinogen as a key regulator of inflammation in disease. *Semin Immunopathol*. 34:43-62.

Desideri, E., R. Vegliante, and M.R. Ciriolo. 2014. Mitochondrial dysfunctions in cancer: Genetic defects and oncogenic signaling impinging on TCA cycle activity. *Cancer letters*.

Dettmer, K., and B.D. Hammock. 2004. Metabolomics--a new exciting field within the "omics" sciences. *Environmental health perspectives*. 112:A396-397.

Eletto, D., D. Eletto, D. Dersh, T. Gidalevitz, and Y. Argon. 2014. Protein Disulfide Isomerase A6 Controls the Decay of IRE1α Signaling via Disulfide-Dependent Association. *Molecular Cell*. 53:562-576.

Fang, L., and Y.I. Miller. 2012. Emerging applications for zebrafish as a model organism to study oxidative mechanisms and their roles in inflammation and vascular accumulation of oxidized lipids. *Free Radical Biology and Medicine*. 53:1411-1420.

Fang, Y., H. Yang, T. Wang, B. Liu, H. Zhao, and M. Chen. 2010. Metallothionein and superoxide dismutase responses to sublethal cadmium exposure in the clam Mactra veneriformis. *Comparative biochemistry and physiology. Toxicology & pharmacology : CBP*. 151:325-333.

Fiehn, O. 2002. Metabolomics--the link between genotypes and phenotypes. *Plant molecular biology*. 48:155-171.

Filipič, M. 2012. Mechanisms of cadmium induced genomic instability. *Mutation Research/Fundamental and Molecular Mechanisms of Mutagenesis*. 733:69-77.

Fuentes-Almagro, C.A., M.J. Prieto-Alamo, C. Pueyo, and J. Jurado. 2012. Identification of proteins containing redox-sensitive thiols after PRDX1, PRDX3 and GCLC silencing and/or glucose oxidase treatment in Hepa 1-6 cells. *Journal of proteomics*. 77:262-279.

Galano, E., A. Arciello, R. Piccoli, D.M. Monti, and A. Amoresano. 2014. A proteomic approach to investigate the effects of cadmium and lead on human primary renal cells. *Metallomics : integrated biometal science*. 6:587-597.

Garcia-Sevillano, M.A., M. Contreras-Acuna, T. Garcia-Barrera, F. Navarro, and J.L. Gomez-Ariza. 2014a. Metabolomic study in plasma, liver and kidney of mice exposed to inorganic arsenic based on mass spectrometry. *Analytical and bioanalytical chemistry*. 406:1455-1469.

Garcia-Sevillano, M.A., T. Garcia-Barrera, N. Abril, C. Pueyo, J. Lopez-Barea, and J.L. Gomez-Ariza. 2014b. Omics technologies and their applications to evaluate metal toxicity in mice M. spretus as a bioindicator. *Journal of proteomics*.

Garcia-Sevillano, M.A., T. Garcia-Barrera, F. Navarro-Roldan, Z. Montero-Lobato, and J.L. Gomez-Ariza. 2014c. A combination of metallomics and metabolomics studies to evaluate the effects of metal interactions in mammals. Application to Mus musculus mice under arsenic/cadmium exposure. *Journal of proteomics*.

Garcia-Sevillano, M.A., T. Garcia-Barrera, F. Navarro, and J.L. Gomez-Ariza. 2013. Analysis of the biological response of mouse liver (Mus musculus) exposed to As2O3 based on integrated -omics approaches. *Metallomics : integrated biometal science*. 5:1644-1655.

Garcia-Sevillano, M.A., M. Gonzalez-Fernandez, R. Jara-Biedma, T. Garcia-Barrera, J. Lopez-Barea, C. Pueyo, and J.L. Gomez-Ariza. 2012. Biological response of free-living mouse Mus spretus from Donana National Park under environmental stress based on assessment of metal-binding biomolecules by SEC-ICP-MS. *Analytical and bioanalytical chemistry*. 404:1967-1981.

Gonzalez-Fernandez, M., T. Garcia-Barrera, J. Jurado, M.J. Prieto-Álamo, C. Pueyo, J. Lopez-Barea, and J.L. Gomez-Ariza. 2008. Integrated application of Transcriptomics, Proteomics and Metallomics in environmental studies. *Pure and Apllied Chemistry*. 12:2609-2626.

Goyer, R.A., and T. Clarkson. 2001. Toxic effects of metals. *In* Casarett and Doull’s Toxicology the Basic Science of Poisons. C.D. Klaassen, editor, Kansas. 811-867. .

Habeebu, S.S., J. Liu, Y. Liu, and C.D. Klaassen. 2000. Metallothionein-null mice are more sensitive than wild-type mice to liver injury induced by repeated exposure to cadmium. *Toxicological sciences : an official journal of the Society of Toxicology*. 55:223-232.

Hamann, I., C. König, C. Richter, G. Jahnke, and A. Hartwig. 2012. Impact of cadmium on hOGG1 and APE1 as a function of the cellular p53 status. *Mutation Research/Fundamental and Molecular Mechanisms of Mutagenesis*. 736:56-63.

Han, E.S., F.L. Muller, V.I. Perez, W. Qi, H. Liang, L. Xi, C. Fu, E. Doyle, M. Hickey, J. Cornell, C.J. Epstein, L.J. Roberts, H. Van Remmen, and A. Richardson. 2008. The in vivo gene expression signature of oxidative stress. *Physiological genomics*. 34:112-126.

Hegde, M.L., T.K. Hazra, and S. Mitra. 2008. Early steps in the DNA base excision/single-strand interruption repair pathway in mammalian cells. *Cell research*. 18:27-47.

Hoeferlin, L.A., B. Fekry, B. Ogretmen, S.A. Krupenko, and N.I. Krupenko. 2013. Folate Stress Induces Apoptosis via p53-dependent de Novo Ceramide Synthesis and Up-regulation of Ceramide Synthase 6. *Journal of Biological Chemistry*. 288:12880-12890.

Jara-Biedma, R., R. Gonzalez-Dominguez, T. Garcia-Barrera, J. Lopez-Barea, C. Pueyo, and J.L. Gomez-Ariza. 2013. Evolution of metallotionein isoforms complexes in hepatic cells of Mus musculus along cadmium exposure. *Biometals : an international journal on the role of metal ions in biology, biochemistry, and medicine*. 26:639-650.

Jihen el, H., H. Fatima, A. Nouha, T. Baati, M. Imed, and K. Abdelhamid. 2010. Cadmium retention increase: a probable key mechanism of the protective effect of zinc on cadmium-induced toxicity in the kidney. *Toxicology letters*. 196:104-109.

Jo, E.J., H.-Y. Lee, Y.-N. Lee, J.I. Kim, H.-K. Kang, D.-W. Park, S.-H. Baek, J.-Y. Kwak, and Y.-S. Bae. 2004. Group IB Secretory Phospholipase A2 Stimulates CXC Chemokine Ligand 8 Production via ERK and NF-κB in Human Neutrophils. *The Journal of Immunology*. 173:6433-6439.

Jozkowicz, A., H. Was, and J. Dulak. 2007. Heme oxygenase-1 in tumors: is it a false friend? *Antioxidants & redox signaling*. 9:2099-2117.

Jurado, J., C.A. Fuentes-Almagro, M.J. Prieto-Alamo, and C. Pueyo. 2007. Alternative splicing of c-fos pre-mRNA: contribution of the rates of synthesis and degradation to the copy number of each transcript isoform and detection of a truncated c-Fos immunoreactive species. *BMC Mol Biol*. 8:83-96.

Jurczuk, M., M.M. Brzoska, J. Rogalska, and J. Moniuszko-Jakoniuk. 2003. Iron body status of rats chronically exposed to cadmium and ethanol. *Alcohol and alcoholism*. 38:202-207.

Jurczuk, M., M. M. Brzóska, J. Moniuszko-Jakoniuk, M. Gałażyn-Sidorczuk, and E. Kulikowska-Karpińska. 2004. Antioxidant enzymes activity and lipid peroxidation in liver and kidney of rats exposed to cadmium and ethanol. *Food and Chemical Toxicology*. 42:429-438.

Kang, H.S., K. Okamoto, Y.S. Kim, Y. Takeda, C.D. Bortner, H. Dang, T. Wada, W. Xie, X.P. Yang, G. Liao, and A.M. Jetten. 2011. Nuclear orphan receptor TAK1/TR4-deficient mice are protected against obesity-linked inflammation, hepatic steatosis, and insulin resistance. *Diabetes*. 60:177-188.

Kensler, T.W., N. Wakabayashi, and S. Biswal. 2007. Cell survival responses to environmental stresses via the Keap1-Nrf2-ARE pathway. *Annual review of pharmacology and toxicology*. 47:89-116.

Kil, I.S., S.W. Shin, H.S. Yeo, Y.S. Lee, and J.-W. Park. 2006. Mitochondrial NADP+-Dependent Isocitrate Dehydrogenase Protects Cadmium-Induced Apoptosis. *Molecular Pharmacology*. 70:1053-1061.

Kim, J.Y., and K. Ozato. 2009. The Sequestosome 1/p62 Attenuates Cytokine Gene Expression in Activated Macrophages by Inhibiting IFN Regulatory Factor 8 and TNF Receptor-Associated Factor 6/NF-κB Activity. *The Journal of Immunology*. 182:2131-2140.

King, M.A., H.D. Halicka, and Z. Darzynkiewicz. 2004. Pro- and anti-apoptotic effects of an inhibitor of chymotrypsin-like serine proteases. *Cell cycle*. 3:1566-1571.

Kothinti, R.K., A.B. Blodgett, D.H. Petering, and N.M. Tabatabai. 2010. Cadmium down-regulation of kidney Sp1 binding to mouse SGLT1 and SGLT2 gene promoters: Possible reaction of cadmium with the zinc finger domain of Sp1. *Toxicology and Applied Pharmacology*. 244:254-262.

Koyu, A., A. Gokcimen, F. Ozguner, D.S. Bayram, and A. Kocak. 2006. Evaluation of the effects of cadmium on rat liver. *Molecular and cellular biochemistry*. 284:81-85.

Larregle, E.V., S.M. Varas, L.B. Oliveros, L.D. Martinez, R. Anton, E. Marchevsky, and M.S. Gimenez. 2008. Lipid metabolism in liver of rat exposed to cadmium. *Food and chemical toxicology : an international journal published for the British Industrial Biological Research Association*. 46:1786-1792.

Lei, T., Q.-Y. He, Z. Cai, Y. Zhou, Y.-L. Wang, L.-S. Si, Z. Cai, and J.-F. Chiu. 2008. Proteomic analysis of chromium cytotoxicity in cultured rat lung epithelial cells. *Proteomics*. 8:2420-2429.

Li, J., and A.S. Lee. 2006. Stress induction of GRP78/BiP and its role in cancer. *Current molecular medicine*. 6:45-54.

Liu, F., K. Inageda, G. Nishitai, and M. Matsuoka. 2006. Cadmium induces the expression of Grp78, an endoplasmic reticulum molecular chaperone, in LLC-PK1 renal epithelial cells. *Environmental health perspectives*. 114:859-864.

Lu, X.J., J. Chen, Z.A. Huang, L. Zhuang, L.Z. Peng, and Y.H. Shi. 2012. Influence of acute cadmium exposure on the liver proteome of a teleost fish, ayu (Plecoglossus altivelis). *Molecular biology reports*. 39:2851-2859.

Ma, Z., H. Izumi, M. Kanai, Y. Kabuyama, N.G. Ahn, and K. Fukasawa. 2006. Mortalin controls centrosome duplication via modulating centrosomal localization of p53. *Oncogene*. 25:5377-5390.

Manna, P., M. Sinha, and P.C. Sil. 2009. Taurine plays a beneficial role against cadmium-induced oxidative renal dysfunction. *Amino acids*. 36:417-428.

Marth, E., S. Jelovcan, B. Kleinhappl, A. Gutschi, and S. Barth. 2001. The effect of heavy metals on the immune system at low concentrations. *International journal of occupational medicine and environmental health*. 14:375-386.

Matovic, V., A. Buha, Z. Bulat, and D. Ethukic-Cosic. 2011. Cadmium toxicity revisited: focus on oxidative stress induction and interactions with zinc and magnesium. *Arh Hig Rada Toksikol*. 62:65-76.

McNeill, D.R., A. Narayana, H.K. Wong, and D.M. Wilson, 3rd. 2004. Inhibition of Ape1 nuclease activity by lead, iron, and cadmium. *Environmental health perspectives*. 112:799-804.

Miyazaki, T., and Y. Matsuzaki. 2014. Taurine and liver diseases: a focus on the heterogeneous protective properties of taurine. *Amino acids*. 46:101-110.

Moniuszko-Jakoniuk, J., M. Jurczuk, M.M. Brzoska, J. Rogalska, and M. Galazyn-Sidorczuk. 2005. Involvement of some low-molecular thiols in the destructive mechanism of cadmium and ethanol action on rat livers and kidneys. *Pol. Environ. Stud.* 14:483–489

Morrison, N., G. Cochrane, N. Faruque, T. Tatusova, Y. Tateno, D. Hancock, and D. Field. 2006. Concept of sample in OMICS technology. *Omics : a journal of integrative biology*. 10:127-137.

Murugavel, P., and L. Pari. 2007a. Diallyl tetrasulfide protects cadmium-induced alterations in lipids and plasma lipoproteins in rats. *Nutrition Research*. 27:356-361.

Murugavel, P., and L. Pari. 2007b. Effects of diallyl tetrasulfide on cadmium-induced oxidative damage in the liver of rats. *Human & experimental toxicology*. 26:527-534.

Nordberg, G.F. 2009. Historical perspectives on cadmium toxicology. *Toxicol Appl Pharmacol*. 238:192-200.

Pelisch, F., B. Pozzi, G. Risso, M.J. Muñoz, and A. Srebrow. 2012. DNA Damage-induced Heterogeneous Nuclear Ribonucleoprotein K SUMOylation Regulates p53 Transcriptional Activation. *Journal of Biological Chemistry*. 287:30789-30799.

Perez-Enciso, M., and M. Tenenhaus. 2003. Prediction of clinical outcome with microarray data: a partial least squares discriminant analysis (PLS-DA) approach. *Human genetics*. 112:581-592.

Prieto-Alamo, M.J., J.M. Cabrera-Luque, and C. Pueyo. 2003. Absolute quantitation of normal and ROS-induced patterns of gene expression: an in vivo real-time PCR study in mice. *Gene Expr*. 11:23-34.

Pueyo, C., J. Jurado, M.J. Prieto-Alamo, F. Monje-Casas, and J. Lopez-Barea. 2002. Multiplex reverse transcription-polymerase chain reaction for determining transcriptional regulation of thioredoxin and glutaredoxin pathways. *Methods in enzymology*. 347:441-451.

Rana, S.V. 2008. Metals and apoptosis: recent developments. *Journal of trace elements in medicine and biology : organ of the Society for Minerals and Trace Elements*. 22:262-284.

Rani, A., A. Kumar, A. Lal, and M. Pant. 2014. Cellular mechanisms of cadmium-induced toxicity: a review. *International journal of environmental health research*. 24:378-399.

Ridgway, N.D. 2013. The role of phosphatidylcholine and choline metabolites to cell proliferation and survival. *Critical reviews in biochemistry and molecular biology*. 48:20-38.

Satarug, S., S.H. Garrett, M.A. Sens, and D.A. Sens. 2010. Cadmium, environmental exposure, and health outcomes. *Environmental health perspectives*. 118:182-190.

Shimada, H., T. Funakoshi, and M.P. Waalkes. 2000. Acute, Nontoxic Cadmium Exposure Inhibits Pancreatic Protease Activities in the Mouse. *Toxicological Sciences*. 53:474-480.

Templeton, D.M., and Y. Liu. 2010. Multiple roles of cadmium in cell death and survival. *Chemico-biological interactions*. 188:267-275.

Tong, W.H., C. Sourbier, G. Kovtunovych, S.Y. Jeong, M. Vira, M. Ghosh, V.V. Romero, R. Sougrat, S. Vaulont, B. Viollet, Y.S. Kim, S. Lee, J. Trepel, R. Srinivasan, G. Bratslavsky, Y. Yang, W.M. Linehan, and T.A. Rouault. 2011. The glycolytic shift in fumarate-hydratase-deficient kidney cancer lowers AMPK levels, increases anabolic propensities and lowers cellular iron levels. *Cancer cell*. 20:315-327.

Tretter, L., and V. Adam-Vizi. 2005. Alpha-ketoglutarate dehydrogenase: a target and generator of oxidative stress. *Philosophical transactions of the Royal Society of London. Series B, Biological sciences*. 360:2335-2345.

Valko, M., H. Morris, and M.T. Cronin. 2005. Metals, toxicity and oxidative stress. *Current medicinal chemistry*. 12:1161-1208.

Wang, L., and E.P. Gallagher. 2013. Role of Nrf2 antioxidant defense in mitigating cadmium-induced oxidative stress in the olfactory system of zebrafish. *Toxicology and Applied Pharmacology*. 266:177-186.

Weckwerth, W. 2010. Metabolomics: an integral technique in systems biology. *Bioanalysis*. 2:829-836.

Wu, K.C., J.J. Liu, and C.D. Klaassen. 2012. Nrf2 activation prevents cadmium-induced acute liver injury. *Toxicology and Applied Pharmacology*. 263:14-20.

Yadav, U.C., and K.V. Ramana. 2013. Regulation of NF-kappaB-induced inflammatory signaling by lipid peroxidation-derived aldehydes. *Oxidative medicine and cellular longevity*. 2013:690545.

Yang, G., C. Biswasa, Q.S. Lin, P. La, F. Namba, T. Zhuang, M. Muthu, and P.A. Dennery. 2013. Heme oxygenase-1 regulates postnatal lung repair after hyperoxia: Role of beta-catenin/hnRNPK signaling. *Redox biology*. 1:234-243.

Zhai, Q., G. Wang, J. Zhao, X. Liu, F. Tian, H. Zhang, and W. Chen. 2013. Protective effects of Lactobacillus plantarum CCFM8610 against acute cadmium toxicity in mice. *Applied and environmental microbiology*. 79:1508-1515.

Zhou, Z., C. Wang, H. Liu, Q. Huang, M. Wang, and Y. Lei. 2013. Cadmium induced cell apoptosis, DNA damage, decreased DNA repair capacity, and genomic instability during malignant transformation of human bronchial epithelial cells. *International journal of medical sciences*. 10:1485-1496.

Figure captions

Figure 1. Lipid peroxidation levels in the liver of Cd treated *Mus musculus* mice compared to control mice. Values are mean ± SD values with 8 mice (3 pools) in each group. All measurements were made in triplicate. Statistical significances were determined with the Student's t-test. Differences between Cd treated mice and the control group were statistically significant at a P value of $\leq$0.0001.

Figure 2. Absolute quantification of transcript molecules in the liver of Cd treated *Mus musculus* mice compared with control mice. Samples were taken after 6 or 10 days of treatment. Values are mean ± SD values with 8 mice in each group. All measurements were made in quadruplicate. Comparisons were made by Student's *t*-test. Statistical significance is expressed as: $***P < 0.001$, $**P < 0.01$ and $*P < 0.05$.

Figure 3. Focal 2-DE gel images showing the differential expression of the 16 identified proteins. Spots with the highest or lowest volume in Cd treated liver mice are shown in **(A)** and **(B)**, respectively. In **(C)** the fold changes in the spot volumes (in arbitrary units) corresponding to 10-days treated mice are given as mean ±SEM from the three gels/dose.

Figure 4. Scores plots of PLS-DA for ESI+ and ESI– ionization modes of polar and lipophilic liver extracts and plasma. Blue diamonds: control mice; red diamonds: 6d Cd-exposed mice; black squares: 10d Cd-exposed mice.

Figure 5. Proposed metabolism of glucose in Cd treated mice. Mitochondrial respiratory dysfunction after Cd exposure results in a switch from oxidative phosphorylation to anaerobic glycolysis (the Warburg effect) and glucose is converted into lactate. The electron transport chain slows down as mitochondrial membrane is depolarized by Cd (Yang, Chen et al. 2007). Some TCA enzymes are Cd/ROS inhibited and citrate is exported to the cytosol and cleaved to acetyl-CoA and oxaloacetate. Acetyl-CoA sustains *de novo* FFA synthesis and oxaloacetate fuels the Krebs cycle. A segment of the TCA cycle still works because glutamate feeds the cycle via α-KG.

Online Supporting Information Available

TITLE: **FUNCTIONAL GENOMICS AND METABOLOMICS REVEAL THE TOXICOLOGICAL EFFECTS OF CADMIUM IN *Mus musculus* MICE**

JOURNAL TITTLE: **Metabolomics**

AUTHORS: **M.A. García-Sevillano[a,b,c,§], N. Abril[d,e,§], R. Fernández-Cisnal[d,e], T. García-Barrera[a,b,c], C. Pueyo[d,e], J. López-Barea[d,e], J.L. Gómez-Ariza[a,b,c,] ***

[a]*Department of Chemistry and Materials Sciences, Faculty of Experimental Science, [e]Agrifood Campus of International Excellence (ceiA3-UHU) and [c]Research Center of Health and Environment (CYSMA), University of Huelva, Campus de El Carmen, 21007-Huelva, SPAIN.*

[d]*Department of Biochemistry and Molecular Biology and [e]Agrifood Campus of International Excellence (ceiA3-UCO), University of Córdoba, Severo Ochoa Building, Rabanales Campus, 14071-Córdoba, SPAIN.*

[§]Both authors contributed equally to this work and should be considered first authors.

***Corresponding Author**: José Luis Gómez Ariza. Tel.: +34 959 219968, fax: +34 959 219942, e-mail address: ariza@uhu.es

As Online Supporting Information are included the following **two** Figure and three Tables:

Supporting Information Figure 1. Experimental design showing the animals per treatment group ant the pooling of the samples for the different assays.

Supporting Information Figure 2. Virtual two-dimensional differential in gel electrophoresis (2D-DIGE) images for comparison of control and 10-days Cd-treated liver mice proteomes. Equal amounts of Cy2 (IS, internal standard with equally mixed samples), Cy5 (control, untreated mice), and Cy3 (10-days Cd treated mice) labeled samples were mixed and then separated on analytical 2D-DIGE. Gels were scanned and a set of Cy5, Cy3, and Cy2 **(A)** images were obtained from each gel. An overlay of three dye scan-images was also obtained **(B)**. The spot intensities and the relative expression ratio were computed using the DeCyder 6.5 software (Amersham Biosciences). Statistical significances were determined with the Student's t-test. As an example, circles in **(B)** mark some spots whose intensities increased (red) or decreased (green) in relation to the IS because of the Cd treatment; for these four spots, the symbol of the identified protein and the fold-change variation (statistically significant at a P value of $\leq$0.05) are indicated and the number assigned to the spot , the Mw and the Ip are given in brackets). The remarked sponts are highlated in **(C)**, where the intensity and direction of the change is also shown.

Supporting Information Table 1. Primers used in this work.

Supporting Information Table 2. Quantification of Cd in liver and plasma of mice by ICP-ORS-MS.

Supporting Information Table 3. Variance in mouse gene expression.

FUNCTIONAL GENOMICS AND METABOLOMICS REVEAL THE TOXICOLOGICAL EFFECTS OF CADMIUM IN *Mus musculus* MICE

M.A. García-Sevillano[a,b,c,§], N. Abril[d,e,§], R. Fernández-Cisnal[d,e], T. García-Barrera[a,b,c], C. Pueyo[d,e], J. López-Barea[d,e], J.L. Gómez-Ariza[a,b,c,] *

[a]Department of Chemistry and Materials Sciences, Faculty of Experimental Science, [e]Agrifood Campus of International Excellence (ceiA3-UHU) and [c]Research Center of Health and Environment (CYSMA), University of Huelva, Campus de El Carmen, 21007-Huelva, SPAIN.

[d]Department of Biochemistry and Molecular Biology and [e]Agrifood Campus of International Excellence (ceiA3-UCO), University of Córdoba, Severo Ochoa Building, Rabanales Campus, 14071-Córdoba, SPAIN.

[§]Both authors contributed equally to this work and should be considered first authors.

***Corresponding Author**: José Luis Gómez Ariza. Tel.: +34 959 219968, fax: +34 959 219942, e-mail address: ariza@uhu.es

Abbreviated title: Toxicological effects of cadmium in mice

Acknowledgements. This project received grants CTM2012-38720-C03-01 and CTM2012-38720-C03-02 from the Ministerio de Economia y Competitividad-Spain; BIO1675, P12-FQM-00442 and P09-FQM-04659 from the Consejería de Innovación, Andalusian government. M.A. García-Sevillano thanks to Ministerio de Educación for a predoctoral grant.

Abstract

Cadmium (Cd) is an environmental pollutant that accumulates in the organisms causing serious health problems. Over the past decades, "*omics*" studies have been conducted trying to elucidate changes in the genome, the transcriptome or the proteome after Cd exposure. Metabolomics is relatively new to the "*omics*" revolution, but has shown enormous potential for investigating biological systems or their perturbations. When metabolomic data are interpreted in combination with genomic, transcriptomic and proteomic results, in the co-called systems biology approach, a holistic knowledge of the organism/process under investigation can be achieved. In this work, transcriptional and proteomic analysis (functional genomics) were combined with metabolomic workflow to evaluate the biological responses caused in *Mus musculus* mice by Cd (subcutaneous injection for 10 consecutive days). Animals showed high Cd levels in liver and plasma, drastic lipid peroxidation in liver, increased transcription of hepatic genes involved in oxidative stress, metal transport, immune response and lipid metabolism and moderate decreases of DNA repair genes mRNAs. 2DE-DIGE proteomics confirmed changes of hepatic proteins related to stress and immune responses, or involved in energy metabolism, suggesting a metabolic switch in the liver from oxidative phosphorylation to aerobic glycolysis, that was confirmed by metabolomics analysis, via DIMS and GC-MS. This metabolic alteration is particularly important for highly proliferating cells, like tumor cells, which require a continuous supply of precursors for the synthesis of lipids, proteins and nucleic acids. The metabolic changes observed in mouse liver by metabolomics and the oxidative stress detected via functional genomics could be in the base of Cd hepatocarcinogenicity.

Keywords: Biological response, qRT-PCR; absolute transcription profiles; 2DE-DIGE proteomics, metabolomics, *Mus musculus*, cadmium exposure, direct infusion mass spectrometry

1. Introduction

Cadmium has become one of the most important environmental pollutants in the world due to its wide application in a variety of industrial processes. Cd accumulates mainly in the liver and kidney and both organs are critical targets for acute Cd toxicity (Goyer and Clarkson, 2001; Jihen el et al., 2010; Nordberg, 2009). Several reports indicate that Cd toxicity involves depletion of reduced glutathione (GSH), inhibition of antioxidant enzymes and of energy metabolism and enhanced production of reactive oxygen species (ROS) (Zhai et al., 2013). Thus, increased lipid peroxidation and oxidative DNA damage, inflammatory processes, apoptosis and necrosis have been described among the mechanisms of Cd-induced liver injury (Afolabi et al., 2012; Asara et al., 2013; Brzoska and Rogalska, 2013; Brzoska et al., 2011; Filipič, 2012; Jihen el et al., 2010; Jurczuk et al., 2003; Jurczuk et al., 2004; Koyu et al., 2006; Matovic et al., 2011; Moniuszko-Jakoniuk et al., 2005; Murugavel and Pari, 2007b; Rana, 2008; Rani et al., 2014; Satarug et al., 2010; Templeton and Liu, 2010).

In recent years, the massive advances in the knowledge of genes and genomes (genomics) prompted the development of several novel "*omics"* very useful to reveal the biological responses of organisms to toxic metal exposure and to understand the toxicity mechanisms of contaminants (Garcia-Sevillano et al., 2014b). Fundamental biological processes can now be studied by applying to one biological sample the full range of "*omics"* technologies (Morrison et al., 2006). Genomics applies methods of Molecular Biology and Bioinformatics to sequence, assemble and analyze the structure and function of genomes (the complete set of DNA within a single cell of an organism). In contrast, Functional Genomics deals with the analysis of gene expression (Transcriptomics) and the comprehensive analysis of proteins/metalloproteins (Proteomics/Metalloproteomics) (Gonzalez-Fernandez et al., 2008). More recently, Metabolomics, the complete study of metabolites involved in different metabolic processes, has become an emerging field in analytical biochemistry and can be regarded as the end point of *"omics"* cascade (Dettmer and Hammock, 2004). Furthermore, since changes in the metabolome are the ultimate response of an organism to genetic alterations or environmental influences, the metabolome is most predictive of phenotype (Fiehn, 2002; Weckwerth, 2010). Thus, the comprehensive and quantitative study of transcripts, proteins and metabolites is an attractive tool for either diagnosing pathology or studying the effects of toxicants on phenotype in the organism under investigation.

Although Cd has been related with several pathologies, the mechanisms underlying Cd toxicity are not yet fully elucidated. We have used here a combination of transcriptomics, proteomics and metabolomics methodologies to obtain a holistic view of the molecular pathways altered by Cd exposure over 10 consecutive days aimed to determine the biochemical consequences for mice. Effects in the hepatic transcriptional profile were measured by absolute quantitative reverse transcription-polymerase chain reaction (qRT-PCR) analysis, combined to 2-DE difference gel electrophoresis (DIGE) to evaluate the perturbations in the liver proteome. These results were complemented with metabolomics data obtained by applying the metabolomic workflow based in the use of molecular mass spectrometry to liver and plasma of *Mus musculus* mice.

2 Materials and methods

2.1 Animal handling

Mus musculus (inbred BALB/c strain) mice were obtained from Charles River Laboratory (Spain). A total of 32 male mice of 7 weeks were allowed to acclimate for 5 days with free access to food and water under controlled conditions (25-30ºC, 12 h light-dark photoperiod) prior to the exposure. For the experiment, mice were distributed into four groups, two being exposed to Cd(II) (as $CdCl_2$) by subcutaneous injection (100 µl) of a solution of 0.1 mg Cd per kg of body weight per day and the other two groups used as control and injected with 100 µL of 0.9% NaCl in ultrapure water. A control and a Cd-treated group of mice were sacrificed at the 6th day of the experience and the other two groups at the 10th day. After being individually anesthetized by isoflurane inhalation, mice were sacrificed by cervical dislocation and exsanguinated by cardiac puncture, dissected using a ceramic scalpel and their organs transferred rapidly to dry ice. Individual organs were weighted in Eppendorf vials, rinsed in 0.9% NaCl solution, frozen in liquid nitrogen and stored at -80 ºC. Individual livers were ground by cryogenic homogenization. Three pools were prepared per experimental condition (control or Cd-treated groups, after 6d and 10d) by mixing equal amounts of homogenized hepatic tissue or plasma from 2-3 mice per pool; each pool represented a biological replicate. The experimental design is pictured in Online Supporting Information Figure 1. Mice were handled according to the norms stipulated by the European Community. The investigation was approved by the Ethics Committees of Córdoba and Huelva Universities (Spain).

2.2 Determination of cadmium concentration in liver and plasma

A SPEX SamplePrep cryogenic homogenizer (Freezer/Mills 6770) was used for solid tissue disruption. Cd concentration was determined in mouse liver and plasma after 6 and 10 days of treatment. Samples (0.100 g) were exactly weighed in 5-ml PTFE microwave vessels and mixed with 500µL of a HNO_3/H_2O_2 mixture (4:1 v/v) (Ultra Trace analytical grade, Fisher Scientific, Leicestershire, UK). After 10 min, the vessels were closed and introduced into a MARS microwave oven (CEM Matthews, NC, USA). The mineralization was carried out at 400 W, starting at room temperature, ramping to 160ºC in 15 min, and holding for 20 min at 160ºC. Then the solutions were made up to 2 g with ultrapure water and trace metals were analyzed with an Agilent 7500ce inductively coupled plasma mass spectrometer

(Agilent Technologies, Tokyo, Japan) equipped with an octopole collision/reaction cell. The element Rh was added as internal standard (1µg /l). All analyses were made using three replicates and previously published operating conditions (Garcia-Sevillano et al., 2012).

2.3 Measurement of lipid peroxidation in liver

Lipid peroxidation was measured as thiobarbituric acid reactive substances (TBARS). Three pools were prepared per each experimental condition (Cd-treated and control groups, after 6d and 10d) by mixing equal amounts of homogenized hepatic tissue ~~or plasma~~ of 2-3 mice per pool; each pool represented biological replicates. Of each sample, 100 mg were disrupted in 300 µL of 10 mM Tris-HCl, pH 7.5, containing 1 mM EDTA, 1 mM GSH and 1 mM PMSF and the lipid peroxides in the homogenate were determined by the Buege and Aust (1978) method with some modifications. Briefly, 2-10 µL of lysates were mixed with 125 µL of 0.5% (w/v) butylated hydroxytoluene in methanol, 50 µL of 0.66 N H_2SO_4 and 37.5 µL of 0.4 M Na_2WO_4, and the total volume was adjusted to 1 mL with water. Samples were vortexed and centrifugated (5000 g, 5 min, at room T) and the supernatant mixed with 250 µL of 1% thiobarbituric acid (w/v in NaOH 0.1M). Mixtures were heated at 95 ºC for 1 hour, cooled to room T in an ice bath, and their fluorescence was determined (Ex/Em 515/550 nm, 15 nm slit width) in a LS 50B fluorescence spectrometer (Perkin Elmer). The TBARS concentrations in each sample were determined from a standard curve generated from 1,1,3,3-tetraethoxypropane and expressed as nmol of MDA formed per 100 mg of tissue. All determinations were carried out in triplicate.

2.4 Absolute quantification of mRNA levels by qRT-PCR

Primer design. Primers directed against mouse *Sod1*, *MT1* and *A170* genes were designed with the Oligo 7.58 software (Molecular Biology Insights) with identical characteristics (Pueyo et al., 2002) to other primers used in this work and previously described (Abril et al., 2014; Fuentes-Almagro et al., 2012; Jurado et al., 2007; Prieto-Alamo et al., 2003). All primers are given in Online Supporting Information Table 1.

RNA sample preparation. Total RNA from individual livers was isolated with the RNeasy Mini Kit (Qiagen) and the resulting RNA was further treated with DNase I (QIAGEN RNase-Free DNase Set) to remove residual DNA. The samples were then cleaned up with the same RNeasy Mini Kit, using the RNA

Clean Up protocol and denatured by heating at 65ºC for 10 min. RNA integrity was determined by microcapillary electrophoresis with the Agilent 2100 Bioanalyzer, and RNA concentrations were accurately measured using the Hellma TrayCell system (Hellma Analytics). Genomic DNA contamination was tested by PCR amplifications of RNA samples without prior cDNA synthesis. Three pools per experimental condition (Cd-treated and control groups after 6 and 10d) were prepared by mixing equal amounts of total RNA of 2-3 mice and used for cDNA synthesis.

qRT-PCR. The absolute quantification of mRNA levels was carried out as described (Jurado et al., 2007). cDNA was generated from 2 µg of pooled RNA and real-time PCR reactions were performed in quadruplicate with 50 ng/well of cDNA. An absolute calibration curve was constructed with 10^2 to 10^9 molecules per well of an *in vitro* synthesized RNA (Jurado et al., 2007; Prieto-Alamo et al., 2003). The number of transcript molecules was calculated from the linear regression of the calibration curve (Jurado et al., 2007; Prieto-Alamo et al., 2003). The reliability of an absolute quantification depends on identical amplification efficiencies for both the target and the calibrator. Our primers were designed to amplify all amplicons with optimal (~100%) efficiencies and high linearity ($r > 0.99$) in the range of 20 to 2×10^5 pg of total RNA input.

2.5 DIGE experiment

Protein extraction. One pool was prepared per each of the two Cd-exposed groups (6 and 10d) by mixing equal amounts of ground liver from the 8 mice included in each group; equal amounts of liver from all control mice were pooled in one unique control (Online Supporting Information Figure 1). From each tissue pool (control, 6d- and 10d-Cd exposed) 100 mg were disrupted in 300 µL of extraction buffer (20 mM Tris-HCl, pH 7.6, containing 0.5 M sucrose, 0.15M KCl, 20 mM DTT, 1 mM PMSF, 6 µM leupeptin and P2714 Sigma Protease Inhibitor after manufacturer´s instructions). Cell debris was cleared by centrifugation (14000 *g*, 10 min, 4ºC) and the supernatants were treated with benzonase (500 U/ml) and ultracentrifuged (105000 *g*, 60 min). These extracts were precipitated by using a 2D-Clean-up kit (GE-Healthcare) after manufacturer's instructions, resuspended in 8 M urea containing 30 mM Tris-HCl and 4% w/v CHAPS and adjusted to pH 8.5. Protein concentration was determined using 2D-Quant Kit (GE Healthcare).

Fluorescent labelling of proteins and 2-DE electrophoresis. Protein samples were labeled using Cy3 and Cy5 dyes (CyDye™ DIGE Fluor minimal, GE Healthcare) after manufacturer's instructions. All samples in the experiment were mixed, labeled with Cy2 dye for use as internal standard (IS) for normalization. Equal amounts (50 μg) of one Cy3 and one Cy5 labeled samples from different experimental conditions and the Cy2-labeled IS were combined and separated on a single 2DE gel (Cy dyes were swapped to compensate for dye differences). Total volume was adjusted to 50 µL, mixed 1:1 with isoelectrofocusing (IEF) rehydration buffer (8 M urea, 4% w/v CHAPS, 130 mM DTT, 2% w/v IPG buffer pH 3-10) and incubated for 30 min to obtain complete denaturation of proteins. All steps were carried out at 4ºC.

Immobilized pH gradient (IPG) strips (pH 4–7, 24 cm) (GE Healthcare) were rehydrated overnight at 20ºC with 390 µl of DeStreack rehydration solution (GE Healthcare) containing 2% w/v of IPG buffer pH 4-7. Then, denatured proteins were cup-loaded in the IPG strips at approximately 1 cm from the cathode. After 6 h active (50 V) rehydration, IEF was carried out (20°C, 50 µA/strip) in a Protean IEF apparatus (Bio-Rad) at 500, 1000, 2000, 4000, 6000 and 8000 V (each 90 min) and 8000 V (until reaching 57 000 Vh). The strips were then soaked 20 min in equilibration mix (50 mM Tris–HCl, pH 8.8, 6 M urea, 30% w/v glycerol, 2% w/v SDS, and bromophenol blue traces) containing 65 mM DTT, drained and again soaked 20 min in this mix containing 0.35 M iodoacetamide. For the second dimension, DryStrips were loaded on top of 12.5% w/v SDS-PAGE gels and separated at 20 °C in a BioRad Protean Plus Dodeca Cell at 2.5 W per gel (10 min) and 3 Wper gel (approx.12 h).

The separated proteins labeled with Cy3, Cy5 and Cy2 dyes were detected in gels using a Typhoon scanner (GE Healthcare). The Cy3- and Cy5-labeled proteins migrating to each 2D spot were quantified based on the corresponding fluorescence intensities and their molar ratios were calculated using the DeCyder 6.5 software (GE Healthcare). Each set of three images from a single gel was first processed using the Differential In-gel Analysis module for automatic spot detection, spot volume quantification and volume ratio normalization of the different samples loaded in the same gel. Then, the Biological Variation Analysis module was used to automatically match the spots among different gels and to identify those showing statistically significant differences between the samples. Statistical analysis (ANOVA) was performed on all spots that exhibited $\geq \pm 1.5$-fold change ($p \leq 0.02$) in protein content.

2.5 In gel digestion and mass spectrometry (MS) analysis

A total of 48 spots corresponding to differentially expressed proteins were selected for identification. Preparative gels were loaded with 300 µg of the IS sample to facilitate matching; protein separation was obtained in the same conditions described above for the DIGE gels. After 2-DE, proteins were stained with Sypro Ruby® (BioRad) according to the manufacturer's instructions, and the selected spots were excised using an Investigator™ProPic station (Genomic Solutions). Spots were destained, dehydrated, and dried. Proteolytic digestion was carried out with 20 µl trypsin (12.5 ng/µl trypsin in 25 mM ammonium bicarbonate) at 25ºC for 10 min followed by 3 x 5 min treatment in a microwave oven (200W). The digestion was stopped by adding 10 ml of 0.5% v/v trifluoroacetic acid (TFA). The resulting peptides were purified in a Pro PrepII station (Genomic Solutions) with a C18 microcolumn (ZipTip, Millipore), eluting with matrix solution (5 mg/ml alpha-Cyano-4-hydroxycinnamic acid in 70% acetonitrile and 0.1% TFA). Samples were directly spotted onto an Opti-TOF® MALDI plate (AB SCIEX) using the Investigator™ ProMS apparatus (Genomic Solutions) and analyzed using an AB SCIEX 4800 MALDI TOF/TOF apparatus, operated in the positive reflection delayed extraction mode. Spectra were internally calibrated using the m/z ratios of the peptides derived from auto-digestion of porcine trypsin (MH 842.509, MH 2211.104). The m/z was measured to a precision of 720 ppm. The MS/MS fragmentation spectra of the most intense 12 m/z fragments were found for each sample. The spectra obtained in the MALDI TOF/TOF analysis, with a signal/noise threshold ≥10, were adjusted to a baseline, deisotoped, and the values of the mono-isotope ions of each peptide were detected.

Molecular masses of the tryptic peptide profiles were used to search in the IPI_Mouse database (http://www.ebi.ac.uk/IPI/IPIhelp.html) with GPS Explorer software v2.0 (Applied Biosystems) and automated database search, using the Mascot Search Engine (Matrix Science). Their masses were compared to the theoretical peptide masses of all available proteins and predicted proteins from DNA sequences. Unmatched peptides were not considered in the analysis. All peptide fragments obtained for each digest were submitted to a search made by combining Peptide Mass Fingerprinting (PMF) and the results from MS/MS fragmentations. Search parameters for the program were as follows: maximum allowed error of peptide mass 100 ppm; cysteine as S-carbamidomethyl-derivative, oxidation of methionine, formation of pyroglutamic acid, and acetylation of the N-terminal extreme allowed.

2.6 Metabolomic workflow

2.6.1 Sample preparation for metabolomics study by mass spectrometry.

All solvents used in sample preparation for the metabolomic study of liver and plasma were of optima LC/MS grade. Methanol, acetonitrile and chloroform were from Fisher Scientific (Leicestershire, UK), while ammonium acetate and formic acid were from Sigma-Aldrich (Steinheim, Germany). Sample preparation of individual livers for metabolomic analysis based on direct infusion to mass spectrometry (DIMS) was carried out in two-steps. 1) *Polar metabolites* were extracted by adding 200 µL of a methanol/acetonitrile mixture (2:1, v/v) to 50 mg tissue in an Eppendorf tube followed by vigorous vortex shaking for 5 min. Then, the cells were disrupted using a pellet mixer (2 min) at 4ºC, and the sample was centrifuged for 10 min at 4000 *g* and 4°C. The supernatant was carefully collected and transferred to another Eppendorf tube. The pellet was re-homogenized as above with 100 µL of methanol/acetonitrile mixture (2:1, v/v), centrifuged as described above and the pellet was kept for further treatment. Both supernatants were combined and stored to -80ºC for analysis. 2) *Lipophilic metabolites* were extracted from the pellet with 200 µL of a chloroform/methanol mixture (2:1, v/v), using a pellet mixer (2 min), and centrifuged at the same conditions described above. The resulting supernatant was stored to -80ºC for analysis.

For DI-ESI(±)-QTOF-MS of blood plasma samples, proteins were removed by adding 400 µL of a methanol/acetonitrile mixture (2:1, v/v) to 100 µL plasma in an Eppendorf tube followed by vigorous vortex shaking for 5 min at room T and centrifugation for 10 min at 4000 *g* and 4 °C. The supernatant was carefully collected avoiding the precipitated proteins, transferred to another Eppendorf tube and the resulting supernatant was taken to dryness under N_2 stream for storage at -80ºC until analysis. To extract lipophilic metabolites, the pellet was homogenized with 200 µL of a chloroform/methanol mixture (2:1, v/v), using a pellet mixer (2 min), and centrifuged for 10 min at 10000 *g* and 4 °C. The resulting supernatant was taken to dryness under N_2 stream and stored at -80ºC for analysis. The polar extracts were reconstituted to 100 µL of a methanol/acetonitrile mixture (2:1, v/v) and the lipophilic extracts were reconstituted to 100 µL of a chloroform/methanol mixture (2:1, v/v) before the analysis by ESI-MS.

For data acquisitions from positive ionization, 0.1 % (v/v) formic acid was added to polar extract and 50 mM of ammonium acetate to lipophilic extract. In the case of negative ionization intact extracts were directly infused to the mass spectrometer.

2.6.2 Analysis of sample extracts by direct infusion-mass spectrometry

Metabolomic experiments of liver and plasma extracts from Cd-exposed mice were performed by DIMS in a QSTAR XL Hybrid system mass spectrometer (Applied Biosystems, Foster City, CA, USA) using an electrospray ionization source (ESI). The parameters for triple quadrupole-time of flight (QqQ-TOF) analyzer were optimized to obtain the higher sensitivity with minimal fragmentation of molecular ions, both in positive and negative ion modes. To acquire MS/MS spectra, N_2 was used as collision gas. Gas chromatography-mass spectrometry (GC-MS) analysis was also applied to mice plasma, as previously described (Garcia-Sevillano et al., 2013). Derivatizing agents, methoxylamine hydrochloride and N-methyl-N-(trimethylsilyl) trifluoroacetamide containing 1% trimethylchlorosilane, were obtained from Sigma-Aldrich.

2.6.3 Analysis of samples by gas chromatography-mass spectrometry

Sample preparation for GC-MS analysis was carried out as a previously published (Garcia-Sevillano et al., 2014a). Separation was performed in a Trace GC ULTRA gas chromatograph coupled to a ITQ900 ion trap mass spectrometer detector, both from Thermo Fisher Scientific, using a Factor Four capillary column VF-5MS 30m×0.25mm ID, with 0.25 µm of film thickness (Varian).

The injector temperature was kept at 280ºC, and He was used as carrier gas at 1 mL/min constant flow rate. For optimal separation, column T was initially maintained at 60ºC for 10 min, and then increased from 60 to 140ºC at a rate of 7 ºC/min and held for 4 min. Then, column T was increased to 180 ºC at 5º C/min and maintained for 6 min. Finally, the T was increased to 320ºC at 5 ºC/min, and held for 2 min. For MS detection, ionization was carried out by electronic impact (EI) with 70 eV voltage, using full scan mode in the m/z range 35–650, with an ion source T of 200ºC. For the analysis, 1 µl of sample was injected in splitless mode. The identification of endogenous metabolites was based on comparison with the corresponding standards according to their retention times and mass spectra characteristics; complementarily, search on NIST Mass Spectral Library (NIST 02) was used.

2.6.4 Data analysis

Markerview™ software (Applied Biosystems) was used to filter the MS results. Statistical data analysis (partial least squares discriminant analysis, PLS-DA) were performed by the SIMCA-P™ statistical software package (v 11.5, UMetrics AB, Umeå, Sweden). PLS-DA is a partial least squares regression of a set Y of binary variables describing the categories of a categorical variable on a set X of predictor variables. It is a compromise between the usual discriminant analysis and a discriminant analysis on the significant principal components of the predictor variables (Perez-Enciso and Tenenhaus, 2003). Data were processed to find differences between mice groups submitted to different exposure time, and to trace the metabolites altered by Cd for later identification by their molecular mass and fragments in

MS/MS experiments. In addition, altered metabolites were characterized using different DIMS-based metabolomics databases, such as Human Metabolome Database (http://www.hmdb.ca), METLIN (http://metlin.scripps.edu) and Mass Bank (http://www.massbank.jp). In GC-MS analysis, metabolite identification was performed using the NIST Mass Spectral Library (NIST 02).

3 Results and discussion

3.1 Determination of cadmium in liver and plasma

The analysis of Cd concentrations in tissue samples revealed a dose-related increase in Cd levels. Male *Mus musculus* mice were daily injected subcutaneously with 0.1 mg Cd per kg of body weight during a total period of 10 days. Data in Online Supporting Information Table 2 shows that Cd accumulation was a gradual process in liver and resulted in >50-fold higher Cd level in the liver of 10d-treated mice compared to the control group, with a >20-fold rise in Cd concentration after 6 days. In plasma a cumulative Cd concentration was found in treated mice, raising from a >12-fold after 6d to >16-fold after 10d, compared to the control group.

3.2 Measurement of lipid peroxidation in liver

Cadmium does not generate free radicals directly, but has been proposed to replace Fe and Cu in various cytoplasmic and membrane proteins. Hence, Cd accumulation in tissues increases the amount of free or chelated Cu and Fe ions participating in oxidative stress via Fenton reactions (Valko et al., 2005). The so generated reactive oxygen species (ROS) cause lipid peroxidation, protein oxidation and DNA damage to the cellular constituents (Fang et al., 2010).

Fig. 1 shows that Cd treatment induced in mice a strong and statistically significant increase of the hepatic MDA levels, a subproduct of lipid peroxidation, according to previous reports (Valko et al., 2005). This MDA increase parallels Cd accumulation in liver and both parameters correlated positively (78.5%) indicating that, irrespectively of the mechanism, Cd caused an intense oxidative stress in the hepatic tissue.

3.3 Transcriptional profile in mouse following cadmium exposure

Both Cd and ROS influence signal transduction processes via the modulation of transcription factors which lead to the transcriptional activation of different genes (Habeebu et al., 2000; Jara-Biedma et al., 2013). Exposure to Cd triggers a cellular antioxidant response via transcriptional regulators, such as the nuclear factor (erythroid-derived 2)-like 2 (Nrf2). Classical Nrf2 target genes are involved in antioxidant defense, including glutathione *S*-transferases, subunits of glutamate–cysteine ligase, heme oxygenase, glutathione peroxidases, peroxiredoxins, and metallothioneins (MT) among others (Kensler et al., 2007; Wu et al., 2012).

Here we have examined in mouse liver the transcriptional responses to Cd exposure, focusing on 14 genes involved in oxidative stress response, metal transport, DNA repair, heat shock response, lipid metabolism and immune response. We worked with three mini-pools prepared by mixing equal amounts of total RNA of 2-3 mice per experimental condition (control and Cd-treated after 6 and 10 days). Since many factors, including animal sacrifice, may contribute to interindividual variability in gene expression, even working with genetically identical mice, we first quantitated by real-time PCR the transcript molecules of three genes, *A170, Mogat1* and *Gpx1* in liver samples of each mouse (8) included in the 6d-control group (Online Supporting Information Table 3). Replicate reactions generated highly reproducible results with SDs <10% of the mean values (<1% of threshold cycle data). Interindividual variations was in the same range, demonstrating that the studied genes have a stable expression in these samples. From these results, we assumed that the study would not be exposed to misinterpretation by using sample pools.

The real-time PCR analysis allowed to accurately assessing the basal expression levels of a selected set of genes in the mice livers, summarized in Figure 2. Genes from low (< 1 mRNA copy/pg of total RNA in the case of *Mogat1*) to high basal expression levels (> 10^3 mRNA copies/pg of total RNA in the case of Gpx1) were determined in a highly quantitative manner. Cd exposure altered the transcript levels of each of the 14 studied genes, chosen as representatives of different stress response pathways, as indicated below.

Stress response

The first set of genes code for the main members of the antioxidant network. SODs dismutate superoxide into O_2 and H_2O_2, subsequently detoxified to H_2O by catalase (CAT) or by members of the glutathione peroxidase (GPX) or peroxiredoxin (PRDX) families (Han et al., 2008). Heme oxygenase 1 (HMO1) disrupts heme, a potent prooxidant and proinflammatory agent, and generates biologically active products such as CO with an important antiinflammatory effect (Jozkowicz et al., 2007). A170, mouse counterpart of the human sequestosome 1 (SQSTM1) or p62, links polyubiquitinated protein aggregates to the autophagic machinery, facilitating their clearance (Bjorkoy et al., 2005). P62/SQSTM1/A170 is a broad negative regulator of cytokine expression that controls the inflammatory response (Kim and Ozato, 2009).

The levels of all these hepatic antioxidant genes rised in a time-dependent manner after Cd exposure, with a significantly higher expression over the control group. Except Gpx1, with a maximum after 6d Cd-treatment, all genes kept rising until 10d exposure. Increases of 2–3 fold over control were found for these 6 genes. Most studies using RT-PCRare are semiquantitative (fold-change) and assume that reference genes are stably expressed, or that any possible changes are balanced. Such assumption biases the interpretation of results, and usually leads to overestimate the role of rare transcripts in the studied process. The absolute expression profiles reported in Figure 2 are not normalized and, thus, do not assume that a reference is steadily expressed. The relevance of data reported here is highlighted when comparing the increments in transcript molecules with the conventional fold variations. Thus, although a 2.32-fold increase in Gpx1 transcripts might look similar to the 2.38-fold rise of Hmo1, the actual scenario is that Gpx1, highly abundant mRNA in liver, exhibited much higher increase in copy number (from ~500 molecules/pg in 6d-control mice to ~1100 molecules/pg in 6d-Cd treated mice) than Hmo1, low abundant mRNA, rising from ~1.4 molecules/pg in 6d-control mice to ~3.3 molecules/pg in 6d-Cd treated mice.

Detoxification of Cd in hepatic cells depends mainly on the induction of metallothioneins (MT), small metal-binding proteins in which 25–30% of all amino acids are cysteine. Cd binds to the thiol groups of MT and is then released by hepatocytes and transported to the kidney in blood plasma. Cd and oxidative stress are particularly strong inducers of MT genes in liver, as reflected in the transcript levels of Mt1 shown in Fig.2. Compared to controls, the livers of Cd-exposed mice showed an impressive and time-dependent increase of Mt-1 mRNA molecules. We have previously reported that Cd exposure also induce MT expression at the protein level, by coupling HPLC with ICP-MS and ESI-MS which permitted us to identify Cd complexes with MT isoforms induced in *Mus musculus* (Jara-Biedma et al., 2013).

Immune response

Cadmium is an immunotoxic that causes disorders in the humoral and cellular immune responses (Afolabi et al., 2012). The first phase of hepatic damage starts by Cd binding to sulfhydryl groups of GSH and proteins, and a second phase is initiated by activation of Kupffer cells, which release proinflammatory cytokines and chemokines (Wu et al., 2012), although the molecular basis for Cd stimulated cytokine expression is unknown. Though Cd specifically induces the transcription of several classes of genes, including those involved in immunity and inflammation, the intermediate events between Cd exposure and induction of cytokine gene expression are not fully defined and may involve numerous pathways (Marth et al., 2001). We found here that Cd caused a strong and sustained rise in the transcript levels of *Pla2g1B* gene reaching 100-fold after 10d treatment (Fig.2). The inflammatory events evoked by pancreatic phospholipase A2, the product of *Pla2g1B,* are thought to be primarily associated with the induction of IL-6 and TNFα from blood monocytes at the transcriptional level (Jo et al., 2004). Hence, *Pla2g1B* induction in liver by Cd might be one of the intermediate events resulting in the induction of cytokine gene expression. Cadmium can also interact with surface structures, inducing the synthesis of immunoglobulins (Igs) (Marth et al., 2001), key humoral components of acquired immunity. A >3-fold increase in the transcripts of Igh gene encoding the Ig heavy chains was observed in the liver of Cd-exposed mice after 10 days (Fig.2), in agreement with the increased IgG and IgM mRNAs described in Cd treated cells (Marth et al., 2001).

DNA repair

DNA damage in Cd-exposed mammalian cells derives from the induction of DNA lesions but also from inactivation of several DNA repair enzymes. BER (base excision repair), key to repair ROS-induced oxidative DNA damage is affected by Cd exposure (Hegde et al., 2008). The mammalian AP-endonuclease, APE1 plays a central role in the BER pathway repairing by DNA glycosylases the apurinic/apyrimidinic (AP) sites generated spontaneously or after excision of oxidized and alkylated bases. The 8-oxoguanine DNA glycosylase 1 (OGG1) repairs 8-oxo-7,8-dihydroguanine, the most frequently formed oxidative DNA base lesion (Hamann et al., 2012). Cadmium extensively decreses the OGG activity in cells and the AP-endonuclease activity from cell extracts or purified APE1 protein (Bravard et al., 2010). Some reports attributed OGG1 and APE1 decrease to diminished transcription of Ogg1 and Ape1 genes, but data are contradictory (Bravard et al., 2010; Hamann et al., 2012; Zhou et al., 2013). Here we confirm that Cd caused a modest decrease in *Ogg1* and *Ape1* transcript molecules, and hence, translational modifications should be the cause of OGG1 and APE1 inhibition described by others (Bravard et al., 2010; Hamann et al., 2012; McNeill et al., 2004).

Lipid metabolism

Though intensively studied in aquatic organisms (i.e., (Fang and Miller, 2012; Lu et al., 2012; Wang and Gallagher, 2013)), there is limited information about the effect of Cd on lipid metabolism in mouse liver. Larregle (Larregle et al., 2008) reported that Cd exposure in rats increased the contents of free fatty acids (FFA), triacylglycerols (TAG) and total cholesterol in liver. The high TAG level in Cd-treated rats was attributed to an increased TAG synthesis. The amounts of mRNA (Fig 2) of two genes, *Mogat1* (~8-fold increase) and *Pla2g1B* (~100-fold increase), suggest that also in the liver of our Cd-treated mice might be higher FFA and TAG levels.

Mogat1 codes for monoacylglycerol acyltransferase-1 active in one of two convergent pathways for TAG biosynthesis, and *Mogat1* up-regulation has been described in mouse models of hepatic steatosis (Cortés et al., 2009; Kang et al., 2011), a major consequence of heavy metal exposure (Garcia-Sevillano et al., 2014c). The *Pla2g1B* induction by Cd (see above) might contribute to the elevate levels of FFA, since PLA2G1B releases fatty acids from dietary phospholipids. The increase in free cholesterol previously observed in the liver of Cd exposed rats (Afolabi et al., 2012; Larregle et al., 2008; Murugavel and Pari, 2007a) has been attributed to enhanced expression of cholesterogenic enzymes including 3-hydroxy-3-methylglutaryl-CoA reductase (HMGCR) and the repression of some cholesterol catabolic pathways. Data in Fig. 2 shown a clear induction at the transcriptional level of *Hmgcr* and *Idi* (isopentenyl-diphosphate delta isomerase 1), two enzymes involved in cholesterol biosynthesis. In fact, *Hmgcr* catalyzes the rate-limiting step in this biosynthetic pathway. The induction of *Hmgcr* might be consequence of *Pla2g1B* induction by Cd and the associated production of IL-6 and TNFα (Murugavel and Pari, 2007b).

The transcriptional analysis reported here draws a global panorama in which Cd caused a strong oxidation of hepatic cells in mice that could not be avoided by the Cd-scavenging action of MT1. The oxidative situation generated affected the lipid metabolism and raised the inflammation response, each being both a cause and effect of the other. Lipids are the main component of cell membranes, and hence alteration of lipid metabolism by Cd might results in alterations in this complex structure.

3.4 Proteomic analysis by DIGE

For the transcriptional study referred above, we selected a group of genes according to the prior knowledge of alterations associated to Cd exposure. Thus, the subsequent results give a directed biological contextualization of their gene signature. An alternative and potentially complementary approach to address this problem is the use of proteomics to assess differences in protein expression profiles. Since the proteome is the protein complement to the genome, proteomic approaches should greatly facilitate the characterization and identification of protein-related changes in mouse liver following Cd administration.

2DE-DIGE analyses were performed in protein extracts from livers of male *Mus musculus* mice daily injected a fixed amount of 0.1 mg Cd/kg of body weight. The livers of mice in each experimental group (6- and 10-days of treatment) were pooled and their proteins extracted. A unique control pool was prepared by mixing equal amounts of homogenized liver from the two control groups. Combinations were made to compare in the same gel each problem pool with any other, labeled with Cy3 in some cases and with Cy5 in others, to correct the dye effect (dye-swapping). The Cy2 dye was used to label the internal standard, obtained by mixing an equal amount of all samples, allowing a significant quantitative comparison of proteomic variations. Six gels were run to achieve a statistically significant measure of the differences in protein expression between the control and the Cd-treated samples. A representative 2D-DIGE gel is depicted in Online Supporting Information Fig. 1. Raw data are accessible from the authors upon request.

The subsequent data analysis detected over 2700 protein spots on each CyDye-labeled gel, in the 4–7 pH range and 14–70 kDa Mr. All protein spots were then quantified, normalized and inter-gel matched. No significant differences were found in mouse liver samples after 2d of Cd exposure, and hence, comparisons were focused on 6d and 10d treated samples. To test for significant differences in protein expression between problem and control samples, the data were filtered using the average volume ratios of ±1.5-fold differences and a t-test p value ≤ 0.02 and assigned to a spot of interest. Forty-eight spots satisfied these requirements and were excised from the gel for subsequent in-gel digestion and MS analysis for protein identification. Data were submitted to MASCOT database search resulting in the identification of 16 proteins (Table 1). Several proteins were found in different isoforms or with different post-translational modifications and then detected in multiple spots, including aldehyde dehydrogenase family 1 member L1 (ALDH1L1, spots 704 and 750) and fibrinogen gamma chain (FGG, spots 1484 and 1500). Among proteins showing significant correlations with Cd concentrations in exposed mice, 5 proteins (7 spots) were up-regulated and 9 down-regulated. The fold-change variation of these 16 spots after 10 consecutive days of Cd-exposure are indicated in Fig. 3.

The identified proteins were submitted to a functional annotation analysis with the Ingenuity Pathway Analysis (IPA®, QIAGEN Redwood City) to unravel their primary role in cell metabolism.

They were grouped into three categories, involved in the *stress response* (7 proteins, 8 spots), the *immune response* (4 proteins, 5 spots) and *energy homeostasis* (3 proteins).

Stress response

Although we initially expected that most proteins deregulated by Cd treatment would have antioxidant functions, other types of stress response genes were predominant (Table 1 and Fig. 3). Most of these proteins have no obvious antioxidant function, except possibly ALDH1L1 (spots 704 and 750) and OAT (ornithine aminotransferase, spot 2597). ALDH1L1 is highly expressed in the liver under Nrf2 control (Abdullah et al., 2012) that regulates the antioxidant response. It is involved in apoptosis (Hoeferlin et al., 2013) and in the detoxification of the intermediate-chain-length aldehydes, byproducts of lipid peroxidation (Yadav and Ramana, 2013). OAT, mainly found in the liver, is a pyridoxal-phosphate dependent mitochondrial matrix aminotransferase involved in the metabolism of ornithine, shown to be up-regulated during ROS-related apoptosis (Lei et al., 2008). Both proteins were up-regulated in the liver of Cd-treated *M.musculus* mice, corroborating the strong oxidative stress detected (Fig. 1) and suggested by the transcriptional data (Fig. 2).

Three protein spots (1091, 1061 and 991), identified as heat shock proteins (GRP78, HSPA9 and TRAP1, respectively) had lower expression in the livers of Cd-treated mice. Cadmium induces the expression of Glucose-regulated protein 78 (GRP78) in certain cell types but not in hepatocytes (Liu et al., 2006). Fig. 3 show that GRP78 was down-regulated in the liver of 10d Cd-exposed mice. This molecular chaperone is a central regulator of the endoplasmic reticulum (ER) function due to its roles in protein folding. GRP78 induction is an important pro-survival component of the unfolded protein response (Li and Lee, 2006) but it is also a restraint to Nrf2 activation (Chang et al., 2012). Down-regulating GRP78 in Cd-treated mice livers might activate the transcription of genes under Nrf2 control, encoding for phase II/III enzymes and the defense against oxidative stress (Chang et al., 2012). Similarly, HSP9 (Heat shock 70kDa protein 9/mortalin/ GRP75) and TRAP1 (tumor necrosis factor receptor associated protein 1) are mitochondrial heat shock cytoprotective proteins related to drug resistance and protection from apoptosis by buffering reactive oxygen species (ROS)-mediated oxidative stress. Their down-regulation in Cd-treated mice probably impaired mitochondrial functions but also enhanced the apoptosis and avoided mitotic defects and chromosome instability in Cd affected hepatic cells (Agorreta et al., 2014; Ma et al., 2006), where DNA repair is compromised as indicated by the decrease in the transcript levels of Ogg1 and Ape1 genes (Fig.2).

PDIA6 (spot 1499), also known as P5 or TXNDC7, is one of more than 20 protein disulfide isomerases (PDIs) in the eukaryotic ER. It is an active oxidoreductase with similar properties to other PDIs, yet it does not seem to be involved directly in protein folding (Eletto et al., 2014). By contrast, PDIA6, limits the duration of the unfolded protein response (UPR) and it has been reported that PDIA6-deficient cells hyperrespond to ER stress, resulting in exaggerated up-regulation of UPR target genes and increased apoptosis (Eletto et al., 2014). All these results suggest that Cd exposure affects genes involved in cell division and particularly mechanisms that are responsible to cell cycle arrest. Our results could indicate that Cd exposure represses hepatocyte division. This hypothesis is further supported by the fact that Cd exposure was also associated with the down-regulation of the heterogeneous nuclear ribonucleoprotein K (hnRNPK, spot 1343), involved in cell signaling and gene expression, cooperating with p53 in transcriptional activation of cell-cycle arrest genes after DNA damage (Pelisch et al., 2012). The loss of hnRNPK in Cd-treated hepatic cells might deregulate genes involved in DNA repair, cell proliferation and apoptosis (Yang et al., 2013). Cadmium has been recently reported (Galano et al., 2014) to interfere with protein folding, leading to accumulation of misfolded proteins and ER stress by decreasing chaperone levels.

Immune response

Increasing evidence demonstrates that Cd induces inflammation (i.e., (Marth et al., 2001)), but its mechanisms remain obscure. Our study showed that Cd exposure was positively associated with the systemic inflammation marker fibrinogen, a soluble glycoprotein synthesized by hepatocytes composed by three distinct polypeptides called Aα, Bβ and γ. Fibrinogen is considered an acute-phase reactant and increased fibrinogen content in the blood is considered an indicator for a proinflammatory state (Davalos and Akassoglou, 2012). Three spots up-regulated by Cd in mouse liver were identified as FGB (spot 1298) and FGG (spots 1484 and 1500). Alpha 1-antitrypsin (AAT) is the archetypal member of the serine proteinase inhibitor (SERPIN) gene family. AAT is an acute-phase reactant and the plasma concentration increases three- to four-fold during the inflammatory response. It has been reported that Cd lowers ATT content and depresses the trypsin inhibitory capacity, an effect not shared with any other divalent ions, Pb, Hg, Ni, Fe, and Zn. Other reports show that in mice Cd inhibits chymotrypsin activity *in vivo*

(Shimada et al., 2000). We found here a down-regulation of ATT isoform Serpin 1c (spot 1562) and chymotrypsinogen B (CTRB, spot 2248) in the liver of Cd-treated mice. Serine proteases inhibition has been described as an integral part of the apoptotic response (King et al., 2004) which agrees with down-regulation of GRP78 and other heat shock proteins. These results would also sustain the pro-inflammatory situation evoked by the increased levels of *Pla2g1B* and *Igh* transcripts (Fig. 2), which probably results in the induction of cytokine gene expression and of the synthesis of immunoglobulins described for Cd (Jo et al., 2004; Marth et al., 2001).

Energy metabolism

Though the energy metabolism class is composed by only 3 proteins, they show great metabolic alterations in the liver of Cd-treated mice. Mitochondrial ATPase synthase b subunit (spot 1532) was down-regulated, suggesting a decreased ATP supply by oxidative phosphorylation during Cd exposure. Phosphoglucomutase (PGM1, spot 1216) that catalyze reversible reactions required for glycolysis and gluconeogenesis was up-regulated in the Cd-treated mice livers, probably to meet the enhanced energy demand caused by Cd and to compensate the decrease of oxidative phosphorylation. Finally, down-regulation of $\Delta(3,5)$-$\Delta(2,4)$-dienoyl-CoA isomerase (ECH), an auxiliary enzyme of unsaturated fatty acid β-oxidation might be related to the dysregulation of lipid metabolism described for Cd toxicity.

3.5 Metabolomic analysis by mass spectrometry

For a better understanding of metabolic disorders caused by Cd exposure, we carried out a metabolomic study in the livers of Cd-exposed mice, in parallel to the transcriptional and proteomic analysis. Considering the highly distinct and diverse features of information obtained at the levels of metabolite, mRNA and protein, the combination of these three approaches should provide a highly comprehensive view on the effects of Cd toxicity.

A partial least squares discriminant analysis (PLS-DA) was performed to discriminate between the groups of mice differentially exposed to Cd, assessing the intensities of the signals in the polar and lipophilic extracts from mice plasma and liver, combining the positive and negative ionization mode of acquisition (Fig. 4). The models built with polar and lipophilic metabolites allow a good classification of samples in the different groups, which are shown by the respective scores plots. The *Variable Influence on the Projection* (VIP) parameter was used to identify the variables responsible for this separation. VIP is a weighted sum of squares of the PLS-DA weight that indicates the importance of the variable to the whole model. Thus, it is possible to select variables with the most significant contribution in discriminating between metabonomic profiles corresponding to exposed groups against controls. Only metabolites with VIP > 1.5 have been considered good biomarkers of Cd exposure. The values of R^2Y (cum) and Q^2 (cum) of the combined model are 0.90-0.95 and 0.80-0.90, respectively, indicating that a combination of datasets between groups provides the best classification and prediction. The complementarity of using both ionization modes for polar and lipophilic metabolites is remarkable (see Table 2). In this sense, some metabolites are ionizable using positive and negative mode of acquisition, such as lysophosphatidylcholines, glucose and glutamate, and others are altered in both extracts, such as phosphatidylcholines (Table 2). As a complementary approach, GC-MS was applied also to confirm and quantify altered metabolites established by DIMS and others that are not possible to ionize by ESI. For this purpose, three derivatizing reagents were used for plasma samples to obtain as much metabolic information as possible. Metabolic profiles of mice plasma samples after 6d and 10d of Cd-exposure were obtained by GC-MS.

Table 2 shows a Cd-induced metabolic deregulation, especially of lipids and glucose metabolism. The livers of Cd treated mice had increased levels of triglycerides (TGs), diglycerides (DGs), free fatty acids (10-18C of different unsaturation degree) and lyso-phosphatidylcholines (LPCs), and higher content of choline, phosphocholine, creatinine, glutamine and lactic acid. In contrast, Cd-exposure decreased the levels of glucose, taurine, glutamate, phenylalanine, creatine, citrate and phosphatidylcholines (PCs) in plasma/liver. Via GC-MS we assessed the plasma content of glucose, isoleucine, glutamate, α-ketoglutarate, phenylalanine, isocitrate and citrate and the increase of lactic acid, glutamine and cholesterol levels, to establish the statistical significance of the variation (Table 2). The metabolic changes observed during Cd exposure can be related to perturbations in different metabolic pathways, as follows:

Carbohydrate metabolism

The levels of energy metabolism intermediates, including glucose and three tricarboxylic acid (TCA) cycle members, citrate, isocitrate and α-ketoglutarate, decrease in mouse liver/plasma under Cd exposure (Table 2). TCA is a core pathway for sugar, lipid, and amino acid metabolism. Besides being responsible for production of reducing cofactors (NADH and $CoQH_2$) which fuel the mitochondrial electron transport chain (ETC) to generate ATP, TCA also provides precursors for biosynthesis of lipid, proteins and nucleic acids (Desideri et al., 2014). It was proposed that Cd exerts its toxic effect mainly blocking the ETC by impairing the electron flow through the cytochrome *bc1* complex (Cannino et al., 2009) (Adiele et al., 2012). Since TCA regulation depends primarily on NAD^+ and ADP availability, ETC blocking would reduce the TCA activity and the concentration of its components. A second, non-excluding, mechanism that can explain the lower levels of some TCA cycle components is the oxidation by Cd of aconitase, isocitrate dehydrogenase (IDH) and α-ketoglutarate dehydrogenase (α-KGDH) enzymes (Kil et al., 2006) (Tretter and Adam-Vizi, 2005), impairing the conversion of citrate in succinyl-CoA; actually these enzymes are very sensitive to oxidative stress. Instead, citrate would be exported to the cytosol and cleaved by ATP-citrate lyase (ACLY) to acetyl-CoA and oxaloacetate. While acetyl-CoA is essential to sustain *de novo* FFA synthesis, oxaloacetate can fuel the Krebs cycle if glutamate is available and feeds the cycle via α-KG (Tretter and Adam-Vizi, 2005) and some generation of NAD(P)H in the Krebs cycle is maintained despite of aconitase being blocked. This segment of the Krebs cycle has been suggested to function in the absence of glucose, such as that we observed in Cd treated mice, and may also explain the low levels of citrate and glutamate (Table 2). It is known that mitochondrial respiratory dysfunction results in a switch from oxidative phosphorylation to aerobic glycolysis (the Warburg effect) (Fig. 5). Increased glycolysis confers growth advantages by diverting glucose to generate NADPH and acetyl-CoA and activates factors involved in fatty acid biosynthesis (Tong et al., 2011). Under this metabolic shift, most of the pyruvate generated from glucose (>90%) is converted to lactate by lactate dehydrogenase to recover the NAD^+ needed to maintain glycolysis, produce ATP and assure cell survival (Desideri et al., 2014). Metabolites quantification (Table 2) suggested the onset of aerobic glycolysis in the liver and plasma of Cd-treated mice. Two other evidences from the proteomic study support this idea. First, the up-regulation of PGM1 (Fig. 3) to assure the provision of glucose to the glycolytic pathway. Second, the down-regulation of TRAP1 (Fig. 3) the mitochondrial chaperone that binds to and inhibits succinate dehydrogenase, may alleviate the inhibition of mitochondrial respiration and promote FA oxidation, TCA cycle intermediates, ATP and enhance cell survival. Large amount of evidence points towards this metabolic shift as being particularly important for highly proliferating cells, like tumor cells, which require a continuous supply of precursors for the synthesis of lipids, proteins and nucleic acids (Desideri et al., 2014). From our results, the drastic metabolic changes observed by metabolomics and the extensive oxidative stress detected via functional genomics approaches could also be in the base of cadmium carcinogenicity.

We realize that the changes we observed in the transcripts, proteins and metabolites levels in mice plasma/liver can be influenced by alterations caused by Cd in other tissues. Nephrotoxicity is one of the main adverse effects of cadmium exposure (Rani et al., 2014), and references herein). As a consequence, Cd resulted in inhibition of glucose uptake by kidney and glucosuria (Kothinti et al., 2010), and references herein), which may be in the origin of the hypoglycemia we detected in plasma by metabolomics (Table 2). Growing epidemiological studies have suggested a possible link between Cd exposure and diabetes as Cd induced oxidative stress causes suppression of insulin secretion and apoptosis in pancreatic islet β-cell (Chang et al., 2013). However, our data showed that cadmium-induced hypoglycemia remains in plasm and indicate that the effects of cadmium on the metabolic routes described in the manuscript (genomics, proteomics and metabolomics findings) may be, at least in part, independent of the hormonal action.

Lipid metabolism

Reprogramming of lipid metabolism, in particular fatty acid synthesis, is an important underlying feature of Cd toxicity. Coupled with changes in glycolysis and the TCA cycle is increased expression of genes encoding key enzymes in FA and cholesterol biosynthesis. Data in Table 2 show that Cd exposure resulted in significantly increased FFA, DGA, TGA and total cholesterol contents in liver/plasma. These results fully agree with those in Fig. 2 indicating that the increased mRNA levels of *Mogat1* (~8-fold), *Pla2g1B* (~100-fold), *Hmgcr* (~3-fold) and *Idi1* (~3-fold) paralleled an increase in the corresponding proteins and lead to lipid metabolism dysregulation. Data also corroborate and extend the knowledge of how Cd increase plasma TGA levels, by rising the hepatic synthesis of TAG and not only by decreased lipoprotein lipase activity that leads to an increase in the circulating triglyceride-rich VLDL (Larregle et al., 2008) (Afolabi et al., 2012). Notice that a lipogenic phenotype is considered as a new hallmark of many cancer cells (Dakubo, 2010). (Desideri et al., 2014).

Membrane lipids are particularly sensitive to free radicals due to the presence of polyunsaturated fatty acids, which preferentially undergo lipid peroxidation. The increased levels of choline and phosphocholine detected in liver and plasma (Table 2) after Cd intake may be associated with Cd induced disruption of cell membranes via peroxidation due to the increased oxidative stress. Phosphatidylcholines (PC) are also major components of biological membranes that incorporate choline as a headgroup, and have an important role in both proliferative growth and programmed cell death. As shown in Table 2, Cd diminished PC levels, what probably can be achieved by increasing the levels of PLA2G1B (see Fig. 2 showing increased transcript levels for Pla2g1b gene) that liberate FA and lyso-PC from PC (Ridgway, 2013).

Amino acid metabolism

Alterations of glucose and amino acid levels seem to be a common response to many toxins in several species. Glutamine is the most abundant naturally occurring amino acid in the body whose metabolism is accelerated during the glucose shift to provide substrates for increased lipogenesis and nucleic acid biosynthesis that are critical to the proliferative cell (Dakubo, 2010). Adaptive accelerated glutamine metabolism imposes an increased glutamine intake that is used mainly (66%) to generate lactate and alanine (Dakubo, 2010). Other metabolites increased under Cd exposure were the amino acids aspartate, valine, glycine and serine, all of them considered gluconeogenic. By contrast, the ketogenic amino acids isoleucine and phenylalanine, were decreased in the liver/plasma of Cd treated mice.

Two small metabolites, taurine and creatine, were decreased in the liver/plasma of Cd-treated mice (Table 2). Taurine (2-aminoethanesulfonic acid), a derivative of cysteine, is the most abundant free amino acid in liver with an important antioxidant role (Manna et al., 2009), that might be linked to the oxidative stress promoted by Cd exposure. It is abundantly maintained in the liver by both endogenous biosynthesis and exogenous transport, but is decreased in liver diseases (Miyazaki and Matsuzaki, 2014). Creatine synthesis requires three amino acids: glycine, methionine and arginine. The decreased levels of creatine in Cd-treated mice livers may be originated by the perturbation of transmethylation caused by the increased choline levels (Table 2). Moreover, carnitine is readily degraded to creatinine to be exported to the urea cycle. Elevation of plasma creatinine concentrations (Table 2) might indicate renal damage.

4 Concluding remarks (200 words max.)

Assessment of metal toxicity in mice requires multi-disciplinary tools to integrate many metabolic pathways and biological responses. "*Omics*" technologies are valuable since they provide massive information about biomolecules in cells and organisms under toxic metals effects. We confirm here that successful application of transcriptional analysis (RT-PCR) of a select group of genes, lipid peroxidation assays, proteomic methods (DIGE) and metabolomic workflow (DIMS and GC-MS) for overall evaluation of Cd-induced perturbations in liver and plasma is due to integration of different *omics*. Our integrated results show a critical effect of Cd on the oxidative status, the immune response, the energy metabolism and the lipid metabolism in the liver of Cd treated *Mus musculus* mice for up to 10 days exposure. Data suggest the occurrence of a metabolic switch from oxidative phosphorylation to aerobic glycolysis. This metabolic alteration is particularly important for highly proliferating cells, like tumor cells, which require a continuous supply of precursors for the synthesis of lipids, proteins and nucleic acids. Hence, the metabolic changes observed by metabolomics and the oxidative stress detected via transcriptional analysis and proteomic methods could also be in the base of Cd carcinogenicity.

Conflict of interest

The authors declare no conflict of interest

Compliance with ethical requirements

Animals were handled according to the directive 2010/63/EU stipulated by the European Community, and the study was approved by the Ethics Committees of University of Córdoba and Huelva Universities (Spain).

References

Abdullah, A., N.R. Kitteringham, R.E. Jenkins, C. Goldring, L. Higgins, M. Yamamoto, J. Hayes, and B.K. Park. 2012. Analysis of the role of Nrf2 in the expression of liver proteins in mice using two-dimensional gel-based proteomics. *Pharmacological reports : PR*. 64:680-697.

Abril, N., J. Ruiz-Laguna, M.A. Garcia-Sevillano, A.M. Mata, J.L. Gomez-Ariza, and C. Pueyo. 2014. Heterologous Microarray Analysis of Transcriptome Alterations in Mus spretus Mice Living in an Industrial Settlement. *Environ Sci Technol*. 48:2183-2192.

Adiele, R.C., D. Stevens, and C. Kamunde. 2012. Differential inhibition of electron transport chain enzyme complexes by cadmium and calcium in isolated rainbow trout (Oncorhynchus mykiss) hepatic mitochondria. *Toxicological sciences : an official journal of the Society of Toxicology*. 127:110-119.

Afolabi, O.K., E.B. Oyewo, A.S. Adekunle, O.T. Adedosu, and A.L. Adedeji. 2012. Impaired lipid levels and inflammatory response in rats exposed to cadmium. *EXCLI Journal* 11:677-687.

Agorreta, J., J. Hu, D. Liu, D. Delia, H. Turley, D.J.P. Ferguson, F. Iborra, M.J. Pajares, M. Larrayoz, I. Zudaire, R. Pio, L.M. Montuenga, A.L. Harris, K. Gatter, and F. Pezzella. 2014. TRAP1 Regulates Proliferation, Mitochondrial Function and has Prognostic Significance in NSCLC. *Molecular Cancer Research*.

Asara, Y., J.A. Marchal, E. Carrasco, H. Boulaiz, G. Solinas, P. Bandiera, M.A. Garcia, C. Farace, A. Montella, and R. Madeddu. 2013. Cadmium modifies the cell cycle and apoptotic profiles of human breast cancer cells treated with 5-fluorouracil. *International journal of molecular sciences*. 14:16600-16616.

Bjorkoy, G., T. Lamark, A. Brech, H. Outzen, M. Perander, A. Overvatn, H. Stenmark, and T. Johansen. 2005. p62/SQSTM1 forms protein aggregates degraded by autophagy and has a protective effect on huntingtin-induced cell death. *The Journal of cell biology*. 171:603-614.

Bravard, A., A. Campalans, M. Vacher, B. Gouget, C. Levalois, S. Chevillard, and J.P. Radicella. 2010. Inactivation by oxidation and recruitment into stress granules of hOGG1 but not APE1 in human cells exposed to sub-lethal concentrations of cadmium. *Mutation Research/Fundamental and Molecular Mechanisms of Mutagenesis*. 685:61-69.

Brzoska, M.M., and J. Rogalska. 2013. Protective effect of zinc supplementation against cadmium-induced oxidative stress and the RANK/RANKL/OPG system imbalance in the bone tissue of rats. *Toxicol Appl Pharmacol*. 272:208-220.

Brzoska, M.M., J. Rogalska, and E. Kupraszewicz. 2011. The involvement of oxidative stress in the mechanisms of damaging cadmium action in bone tissue: a study in a rat model of moderate and relatively high human exposure. *Toxicol Appl Pharmacol*. 250:327-335.

Cannino, G., E. Ferruggia, C. Luparello, and A.M. Rinaldi. 2009. Cadmium and mitochondria. *Mitochondrion*. 9:377-384.

Cortés, V.A., D.E. Curtis, S. Sukumaran, X. Shao, V. Parameswara, S. Rashid, A.R. Smith, J. Ren, V. Esser, R.E. Hammer, A.K. Agarwal, J.D. Horton, and A. Garg. 2009. Molecular mechanisms of hepatic steatosis and insulin resistance in the AGPAT2-deficient mouse model of congenital generalized lipodystrophy. *Cell metabolism*. 9:165-176.

Chang, K.-C., C.-C. Hsu, S.-H. Liu, C.-C. Su, C.-C. Yen, M.-J. Lee, K.-L. Chen, T.-J. Ho, D.-Z. Hung, C.-C. Wu, T.-H. Lu, Y.-C. Su, Y.-W. Chen, and C.-F. Huang. 2013. Cadmium Induces Apoptosis in Pancreatic β-Cells through a Mitochondria-Dependent Pathway: The Role of Oxidative Stress-Mediated c-Jun N-Terminal Kinase Activation. *PLoS ONE*. 8:e54374.

Chang, Y.J., Y.P. Huang, Z.L. Li, and C.H. Chen. 2012. GRP78 knockdown enhances apoptosis via the down-regulation of oxidative stress and Akt pathway after epirubicin treatment in colon cancer DLD-1 cells. *PLoS One*. 7:e35123.

Dakubo, G.D. 2010. The Warburg Phenomenon and Other Metabolic Alterations of Cancer Cells. *In* Mitochondrial Genetics and Cancer. Springer-Verlag, Berlin, Heidelberg.

Davalos, D., and K. Akassoglou. 2012. Fibrinogen as a key regulator of inflammation in disease. *Semin Immunopathol*. 34:43-62.

Desideri, E., R. Vegliante, and M.R. Ciriolo. 2014. Mitochondrial dysfunctions in cancer: Genetic defects and oncogenic signaling impinging on TCA cycle activity. *Cancer letters*.

Dettmer, K., and B.D. Hammock. 2004. Metabolomics--a new exciting field within the "omics" sciences. *Environmental health perspectives*. 112:A396-397.

Eletto, D., D. Eletto, D. Dersh, T. Gidalevitz, and Y. Argon. 2014. Protein Disulfide Isomerase A6 Controls the Decay of IRE1α Signaling via Disulfide-Dependent Association. *Molecular Cell*. 53:562-576.

Fang, L., and Y.I. Miller. 2012. Emerging applications for zebrafish as a model organism to study oxidative mechanisms and their roles in inflammation and vascular accumulation of oxidized lipids. *Free Radical Biology and Medicine*. 53:1411-1420.

Fang, Y., H. Yang, T. Wang, B. Liu, H. Zhao, and M. Chen. 2010. Metallothionein and superoxide dismutase responses to sublethal cadmium exposure in the clam Mactra veneriformis. *Comparative biochemistry and physiology. Toxicology & pharmacology : CBP*. 151:325-333.

Fiehn, O. 2002. Metabolomics--the link between genotypes and phenotypes. *Plant molecular biology*. 48:155-171.

Filipič, M. 2012. Mechanisms of cadmium induced genomic instability. *Mutation Research/Fundamental and Molecular Mechanisms of Mutagenesis*. 733:69-77.

Fuentes-Almagro, C.A., M.J. Prieto-Alamo, C. Pueyo, and J. Jurado. 2012. Identification of proteins containing redox-sensitive thiols after PRDX1, PRDX3 and GCLC silencing and/or glucose oxidase treatment in Hepa 1-6 cells. *Journal of proteomics*. 77:262-279.

Galano, E., A. Arciello, R. Piccoli, D.M. Monti, and A. Amoresano. 2014. A proteomic approach to investigate the effects of cadmium and lead on human primary renal cells. *Metallomics : integrated biometal science*. 6:587-597.

Garcia-Sevillano, M.A., M. Contreras-Acuna, T. Garcia-Barrera, F. Navarro, and J.L. Gomez-Ariza. 2014a. Metabolomic study in plasma, liver and kidney of mice exposed to inorganic arsenic based on mass spectrometry. *Analytical and bioanalytical chemistry*. 406:1455-1469.

Garcia-Sevillano, M.A., T. Garcia-Barrera, N. Abril, C. Pueyo, J. Lopez-Barea, and J.L. Gomez-Ariza. 2014b. Omics technologies and their applications to evaluate metal toxicity in mice M. spretus as a bioindicator. *Journal of proteomics*.

Garcia-Sevillano, M.A., T. Garcia-Barrera, F. Navarro-Roldan, Z. Montero-Lobato, and J.L. Gomez-Ariza. 2014c. A combination of metallomics and metabolomics studies to evaluate the effects of metal interactions in mammals. Application to Mus musculus mice under arsenic/cadmium exposure. *Journal of proteomics*.

Garcia-Sevillano, M.A., T. Garcia-Barrera, F. Navarro, and J.L. Gomez-Ariza. 2013. Analysis of the biological response of mouse liver (Mus musculus) exposed to As2O3 based on integrated -omics approaches. *Metallomics : integrated biometal science*. 5:1644-1655.

Garcia-Sevillano, M.A., M. Gonzalez-Fernandez, R. Jara-Biedma, T. Garcia-Barrera, J. Lopez-Barea, C. Pueyo, and J.L. Gomez-Ariza. 2012. Biological response of free-living mouse Mus spretus from Donana National Park under environmental stress based on assessment of metal-binding biomolecules by SEC-ICP-MS. *Analytical and bioanalytical chemistry*. 404:1967-1981.

Gonzalez-Fernandez, M., T. Garcia-Barrera, J. Jurado, M.J. Prieto-Álamo, C. Pueyo, J. Lopez-Barea, and J.L. Gomez-Ariza. 2008. Integrated application of Transcriptomics, Proteomics and Metallomics in environmental studies. *Pure and Apllied Chemistry*. 12:2609-2626.

Goyer, R.A., and T. Clarkson. 2001. Toxic effects of metals. *In* Casarett and Doull's Toxicology the Basic Science of Poisons. C.D. Klaassen, editor, Kansas. 811-867. .

Habeebu, S.S., J. Liu, Y. Liu, and C.D. Klaassen. 2000. Metallothionein-null mice are more sensitive than wild-type mice to liver injury induced by repeated exposure to cadmium. *Toxicological sciences : an official journal of the Society of Toxicology*. 55:223-232.

Hamann, I., C. König, C. Richter, G. Jahnke, and A. Hartwig. 2012. Impact of cadmium on hOGG1 and APE1 as a function of the cellular p53 status. *Mutation Research/Fundamental and Molecular Mechanisms of Mutagenesis*. 736:56-63.

Han, E.S., F.L. Muller, V.I. Perez, W. Qi, H. Liang, L. Xi, C. Fu, E. Doyle, M. Hickey, J. Cornell, C.J. Epstein, L.J. Roberts, H. Van Remmen, and A. Richardson. 2008. The in vivo gene expression signature of oxidative stress. *Physiological genomics*. 34:112-126.

Hegde, M.L., T.K. Hazra, and S. Mitra. 2008. Early steps in the DNA base excision/single-strand interruption repair pathway in mammalian cells. *Cell research*. 18:27-47.

Hoeferlin, L.A., B. Fekry, B. Ogretmen, S.A. Krupenko, and N.I. Krupenko. 2013. Folate Stress Induces Apoptosis via p53-dependent de Novo Ceramide Synthesis and Up-regulation of Ceramide Synthase 6. *Journal of Biological Chemistry*. 288:12880-12890.

Jara-Biedma, R., R. Gonzalez-Dominguez, T. Garcia-Barrera, J. Lopez-Barea, C. Pueyo, and J.L. Gomez-Ariza. 2013. Evolution of metallotionein isoforms complexes in hepatic cells of Mus musculus along cadmium exposure. *Biometals : an international journal on the role of metal ions in biology, biochemistry, and medicine*. 26:639-650.

Jihen el, H., H. Fatima, A. Nouha, T. Baati, M. Imed, and K. Abdelhamid. 2010. Cadmium retention increase: a probable key mechanism of the protective effect of zinc on cadmium-induced toxicity in the kidney. *Toxicology letters*. 196:104-109.

Jo, E.J., H.-Y. Lee, Y.-N. Lee, J.I. Kim, H.-K. Kang, D.-W. Park, S.-H. Baek, J.-Y. Kwak, and Y.-S. Bae. 2004. Group IB Secretory Phospholipase A2 Stimulates CXC Chemokine Ligand 8 Production via ERK and NF-κB in Human Neutrophils. *The Journal of Immunology*. 173:6433-6439.

Jozkowicz, A., H. Was, and J. Dulak. 2007. Heme oxygenase-1 in tumors: is it a false friend? *Antioxidants & redox signaling*. 9:2099-2117.

Jurado, J., C.A. Fuentes-Almagro, M.J. Prieto-Alamo, and C. Pueyo. 2007. Alternative splicing of c-fos pre-mRNA: contribution of the rates of synthesis and degradation to the copy number of each transcript isoform and detection of a truncated c-Fos immunoreactive species. *BMC Mol Biol*. 8:83-96.

Jurczuk, M., M.M. Brzoska, J. Rogalska, and J. Moniuszko-Jakoniuk. 2003. Iron body status of rats chronically exposed to cadmium and ethanol. *Alcohol and alcoholism*. 38:202-207.

Jurczuk, M., M. M. Brzóska, J. Moniuszko-Jakoniuk, M. Gałażyn-Sidorczuk, and E. Kulikowska-Karpińska. 2004. Antioxidant enzymes activity and lipid peroxidation in liver and kidney of rats exposed to cadmium and ethanol. *Food and Chemical Toxicology*. 42:429-438.

Kang, H.S., K. Okamoto, Y.S. Kim, Y. Takeda, C.D. Bortner, H. Dang, T. Wada, W. Xie, X.P. Yang, G. Liao, and A.M. Jetten. 2011. Nuclear orphan receptor TAK1/TR4-deficient mice are protected against obesity-linked inflammation, hepatic steatosis, and insulin resistance. *Diabetes*. 60:177-188.

Kensler, T.W., N. Wakabayashi, and S. Biswal. 2007. Cell survival responses to environmental stresses via the Keap1-Nrf2-ARE pathway. *Annual review of pharmacology and toxicology*. 47:89-116.

Kil, I.S., S.W. Shin, H.S. Yeo, Y.S. Lee, and J.-W. Park. 2006. Mitochondrial NADP+-Dependent Isocitrate Dehydrogenase Protects Cadmium-Induced Apoptosis. *Molecular Pharmacology*. 70:1053-1061.

Kim, J.Y., and K. Ozato. 2009. The Sequestosome 1/p62 Attenuates Cytokine Gene Expression in Activated Macrophages by Inhibiting IFN Regulatory Factor 8 and TNF Receptor-Associated Factor 6/NF-κB Activity. *The Journal of Immunology*. 182:2131-2140.

King, M.A., H.D. Halicka, and Z. Darzynkiewicz. 2004. Pro- and anti-apoptotic effects of an inhibitor of chymotrypsin-like serine proteases. *Cell cycle*. 3:1566-1571.

Kothinti, R.K., A.B. Blodgett, D.H. Petering, and N.M. Tabatabai. 2010. Cadmium down-regulation of kidney Sp1 binding to mouse SGLT1 and SGLT2 gene promoters: Possible reaction of cadmium with the zinc finger domain of Sp1. *Toxicology and Applied Pharmacology*. 244:254-262.

Koyu, A., A. Gokcimen, F. Ozguner, D.S. Bayram, and A. Kocak. 2006. Evaluation of the effects of cadmium on rat liver. *Molecular and cellular biochemistry*. 284:81-85.

Larregle, E.V., S.M. Varas, L.B. Oliveros, L.D. Martinez, R. Anton, E. Marchevsky, and M.S. Gimenez. 2008. Lipid metabolism in liver of rat exposed to cadmium. *Food and chemical toxicology : an international journal published for the British Industrial Biological Research Association*. 46:1786-1792.

Lei, T., Q.-Y. He, Z. Cai, Y. Zhou, Y.-L. Wang, L.-S. Si, Z. Cai, and J.-F. Chiu. 2008. Proteomic analysis of chromium cytotoxicity in cultured rat lung epithelial cells. *Proteomics*. 8:2420-2429.

Li, J., and A.S. Lee. 2006. Stress induction of GRP78/BiP and its role in cancer. *Current molecular medicine*. 6:45-54.

Liu, F., K. Inageda, G. Nishitai, and M. Matsuoka. 2006. Cadmium induces the expression of Grp78, an endoplasmic reticulum molecular chaperone, in LLC-PK1 renal epithelial cells. *Environmental health perspectives*. 114:859-864.

Lu, X.J., J. Chen, Z.A. Huang, L. Zhuang, L.Z. Peng, and Y.H. Shi. 2012. Influence of acute cadmium exposure on the liver proteome of a teleost fish, ayu (Plecoglossus altivelis). *Molecular biology reports*. 39:2851-2859.

Ma, Z., H. Izumi, M. Kanai, Y. Kabuyama, N.G. Ahn, and K. Fukasawa. 2006. Mortalin controls centrosome duplication via modulating centrosomal localization of p53. *Oncogene*. 25:5377-5390.

Manna, P., M. Sinha, and P.C. Sil. 2009. Taurine plays a beneficial role against cadmium-induced oxidative renal dysfunction. *Amino acids*. 36:417-428.

Marth, E., S. Jelovcan, B. Kleinhappl, A. Gutschi, and S. Barth. 2001. The effect of heavy metals on the immune system at low concentrations. *International journal of occupational medicine and environmental health*. 14:375-386.

Matovic, V., A. Buha, Z. Bulat, and D. Ethukic-Cosic. 2011. Cadmium toxicity revisited: focus on oxidative stress induction and interactions with zinc and magnesium. *Arh Hig Rada Toksikol*. 62:65-76.

McNeill, D.R., A. Narayana, H.K. Wong, and D.M. Wilson, 3rd. 2004. Inhibition of Ape1 nuclease activity by lead, iron, and cadmium. *Environmental health perspectives*. 112:799-804.

Miyazaki, T., and Y. Matsuzaki. 2014. Taurine and liver diseases: a focus on the heterogeneous protective properties of taurine. *Amino acids*. 46:101-110.

Moniuszko-Jakoniuk, J., M. Jurczuk, M.M. Brzoska, J. Rogalska, and M. Galazyn-Sidorczuk. 2005. Involvement of some low-molecular thiols in the destructive mechanism of cadmium and ethanol action on rat livers and kidneys. *Pol. Environ. Stud.* 14:483–489

Morrison, N., G. Cochrane, N. Faruque, T. Tatusova, Y. Tateno, D. Hancock, and D. Field. 2006. Concept of sample in OMICS technology. *Omics : a journal of integrative biology*. 10:127-137.

Murugavel, P., and L. Pari. 2007a. Diallyl tetrasulfide protects cadmium-induced alterations in lipids and plasma lipoproteins in rats. *Nutrition Research*. 27:356-361.

Murugavel, P., and L. Pari. 2007b. Effects of diallyl tetrasulfide on cadmium-induced oxidative damage in the liver of rats. *Human & experimental toxicology*. 26:527-534.

Nordberg, G.F. 2009. Historical perspectives on cadmium toxicology. *Toxicol Appl Pharmacol*. 238:192-200.

Pelisch, F., B. Pozzi, G. Risso, M.J. Muñoz, and A. Srebrow. 2012. DNA Damage-induced Heterogeneous Nuclear Ribonucleoprotein K SUMOylation Regulates p53 Transcriptional Activation. *Journal of Biological Chemistry*. 287:30789-30799.

Perez-Enciso, M., and M. Tenenhaus. 2003. Prediction of clinical outcome with microarray data: a partial least squares discriminant analysis (PLS-DA) approach. *Human genetics*. 112:581-592.

Prieto-Alamo, M.J., J.M. Cabrera-Luque, and C. Pueyo. 2003. Absolute quantitation of normal and ROS-induced patterns of gene expression: an in vivo real-time PCR study in mice. *Gene Expr*. 11:23-34.

Pueyo, C., J. Jurado, M.J. Prieto-Alamo, F. Monje-Casas, and J. Lopez-Barea. 2002. Multiplex reverse transcription-polymerase chain reaction for determining transcriptional regulation of thioredoxin and glutaredoxin pathways. *Methods in enzymology*. 347:441-451.

Rana, S.V. 2008. Metals and apoptosis: recent developments. *Journal of trace elements in medicine and biology : organ of the Society for Minerals and Trace Elements*. 22:262-284.

Rani, A., A. Kumar, A. Lal, and M. Pant. 2014. Cellular mechanisms of cadmium-induced toxicity: a review. *International journal of environmental health research*. 24:378-399.

Ridgway, N.D. 2013. The role of phosphatidylcholine and choline metabolites to cell proliferation and survival. *Critical reviews in biochemistry and molecular biology*. 48:20-38.

Satarug, S., S.H. Garrett, M.A. Sens, and D.A. Sens. 2010. Cadmium, environmental exposure, and health outcomes. *Environmental health perspectives*. 118:182-190.

Shimada, H., T. Funakoshi, and M.P. Waalkes. 2000. Acute, Nontoxic Cadmium Exposure Inhibits Pancreatic Protease Activities in the Mouse. *Toxicological Sciences*. 53:474-480.

Templeton, D.M., and Y. Liu. 2010. Multiple roles of cadmium in cell death and survival. *Chemico-biological interactions*. 188:267-275.

Tong, W.H., C. Sourbier, G. Kovtunovych, S.Y. Jeong, M. Vira, M. Ghosh, V.V. Romero, R. Sougrat, S. Vaulont, B. Viollet, Y.S. Kim, S. Lee, J. Trepel, R. Srinivasan, G. Bratslavsky, Y. Yang, W.M. Linehan, and T.A. Rouault. 2011. The glycolytic shift in fumarate-hydratase-deficient kidney cancer lowers AMPK levels, increases anabolic propensities and lowers cellular iron levels. *Cancer cell*. 20:315-327.

Tretter, L., and V. Adam-Vizi. 2005. Alpha-ketoglutarate dehydrogenase: a target and generator of oxidative stress. *Philosophical transactions of the Royal Society of London. Series B, Biological sciences*. 360:2335-2345.

Valko, M., H. Morris, and M.T. Cronin. 2005. Metals, toxicity and oxidative stress. *Current medicinal chemistry*. 12:1161-1208.

Wang, L., and E.P. Gallagher. 2013. Role of Nrf2 antioxidant defense in mitigating cadmium-induced oxidative stress in the olfactory system of zebrafish. *Toxicology and Applied Pharmacology*. 266:177-186.

Weckwerth, W. 2010. Metabolomics: an integral technique in systems biology. *Bioanalysis*. 2:829-836.

Wu, K.C., J.J. Liu, and C.D. Klaassen. 2012. Nrf2 activation prevents cadmium-induced acute liver injury. *Toxicology and Applied Pharmacology*. 263:14-20.

Yadav, U.C., and K.V. Ramana. 2013. Regulation of NF-kappaB-induced inflammatory signaling by lipid peroxidation-derived aldehydes. *Oxidative medicine and cellular longevity*. 2013:690545.

Yang, G., C. Biswasa, Q.S. Lin, P. La, F. Namba, T. Zhuang, M. Muthu, and P.A. Dennery. 2013. Heme oxygenase-1 regulates postnatal lung repair after hyperoxia: Role of beta-catenin/hnRNPK signaling. *Redox biology*. 1:234-243.

Zhai, Q., G. Wang, J. Zhao, X. Liu, F. Tian, H. Zhang, and W. Chen. 2013. Protective effects of Lactobacillus plantarum CCFM8610 against acute cadmium toxicity in mice. *Applied and environmental microbiology*. 79:1508-1515.

Zhou, Z., C. Wang, H. Liu, Q. Huang, M. Wang, and Y. Lei. 2013. Cadmium induced cell apoptosis, DNA damage, decreased DNA repair capacity, and genomic instability during malignant transformation of human bronchial epithelial cells. *International journal of medical sciences*. 10:1485-1496.

Figure captions

Figure 1. Lipid peroxidation levels in the liver of Cd treated *Mus musculus* mice compared to control mice. Values are mean ± SD values with 8 mice (3 pools) in each group. All measurements were made in triplicate. Statistical significances were determined with the Student's t-test. Differences between Cd treated mice and the control group were statistically significant at a P value of ≤ 0.0001.

Figure 2. Absolute quantification of transcript molecules in the liver of Cd treated *Mus musculus* mice compared with control mice. Samples were taken after 6 or 10 days of treatment. Values are mean ± SD values with 8 mice in each group. All measurements were made in quadruplicate. Comparisons were made by Student's *t*-test. Statistical significance is expressed as: ***$P < 0.001$, **$P < 0.01$ and *$P < 0.05$.

Figure 3. Focal 2-DE gel images showing the differential expression of the 16 identified proteins. Spots with the highest or lowest volume in Cd treated liver mice are shown in **(A)** and **(B)**, respectively. In **(C)** the fold changes in the spot volumes (in arbitrary units) corresponding to 10-days treated mice are given as mean ±SEM from the three gels/dose.

Figure 4. Scores plots of PLS-DA for ESI+ and ESI– ionization modes of polar and lipophilic liver extracts and plasma. Blue diamonds: control mice; red diamonds: 6d Cd-exposed mice; black squares: 10d Cd-exposed mice.

Figure 5. Proposed metabolism of glucose in Cd treated mice. Mitochondrial respiratory dysfunction after Cd exposure results in a switch from oxidative phosphorylation to anaerobic glycolysis (the Warburg effect) and glucose is converted into lactate. The electron transport chain slows down as mitochondrial membrane is depolarized by Cd (Yang, Chen et al. 2007). Some TCA enzymes are Cd/ROS inhibited and citrate is exported to the cytosol and cleaved to acetyl-CoA and oxaloacetate. Acetyl-CoA sustains *de novo* FFA synthesis and oxaloacetate fuels the Krebs cycle. A segment of the TCA cycle still works because glutamate feeds the cycle via α-KG.

Online Supporting Information Available

TITLE: **FUNCTIONAL GENOMICS AND METABOLOMICS REVEAL THE TOXICOLOGICAL EFFECTS OF CADMIUM IN *Mus musculus* MICE**

JOURNAL TITTLE: **Metabolomics**

AUTHORS: **M.A. García-Sevillano[a,b,c,§], N. Abril[d,e,§], R. Fernández-Cisnal[d,e], T. García-Barrera[a,b,c], C. Pueyo[d,e], J. López-Barea[d,e], J.L. Gómez-Ariza[a,b,c,] ***

[a]Department of Chemistry and Materials Sciences, Faculty of Experimental Science, [e]Agrifood Campus of International Excellence (ceiA3-UHU) and [c]Research Center of Health and Environment (CYSMA), University of Huelva, Campus de El Carmen, 21007-Huelva, SPAIN.

[d]Department of Biochemistry and Molecular Biology and [e]Agrifood Campus of International Excellence (ceiA3-UCO), University of Córdoba, Severo Ochoa Building, Rabanales Campus, 14071-Córdoba, SPAIN.

[§]Both authors contributed equally to this work and should be considered first authors.

***Corresponding Author**: José Luis Gómez Ariza. Tel.: +34 959 219968, fax: +34 959 219942, e-mail address: ariza@uhu.es

As Online Supporting Information are included the following **two** Figure and three Tables:

Supporting Information Figure 1. Experimental design showing the animals per treatment group ant the pooling of the samples for the different assays.

Supporting Information Figure 2. Virtual two-dimensional differential in gel electrophoresis (2D-DIGE) images for comparison of control and 10-days Cd-treated liver mice proteomes. Equal amounts of Cy2 (IS, internal standard with equally mixed samples), Cy5 (control, untreated mice), and Cy3 (10-days Cd treated mice) labeled samples were mixed and then separated on analytical 2D-DIGE. Gels were scanned and a set of Cy5, Cy3, and Cy2 **(A)** images were obtained from each gel. An overlay of three dye scan-images was also obtained **(B)**. The spot intensities and the relative expression ratio were computed using the DeCyder 6.5 software (Amersham Biosciences). Statistical significances were determined with the Student's t-test. As an example, circles in **(B)** mark some spots whose intensities increased (red) or decreased (green) in relation to the IS because of the Cd treatment; for these four spots, the symbol of the identified protein and the fold-change variation (statistically significant at a P value of ≤ 0.05) are indicated and the number assigned to the spot , the Mw and the Ip are given in brackets). The remarked sponts are highlated in **(C)**, where the intensity and direction of the change is also shown.

Supporting Information Table 1. Primers used in this work.

Supporting Information Table 2. Quantification of Cd in liver and plasma of mice by ICP-ORS-MS.

Supporting Information Table 3. Variance in mouse gene expression.

Figure 1
Click here to download high resolution image

Figure 1.

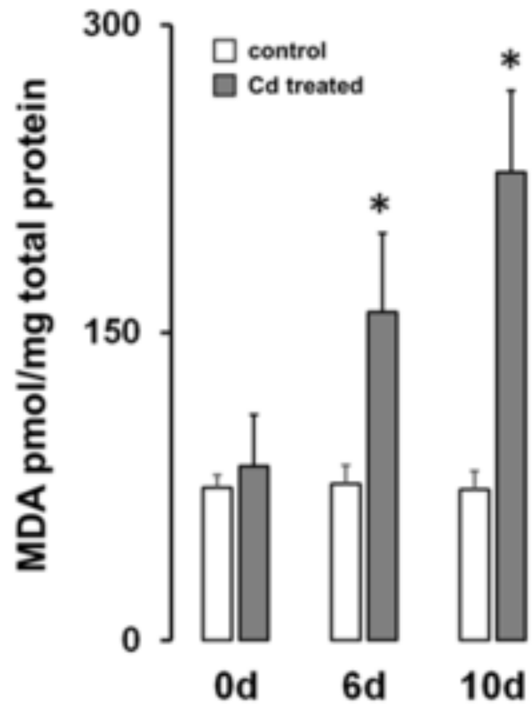

Figure 2
Click here to download high resolution image

Figure 2.

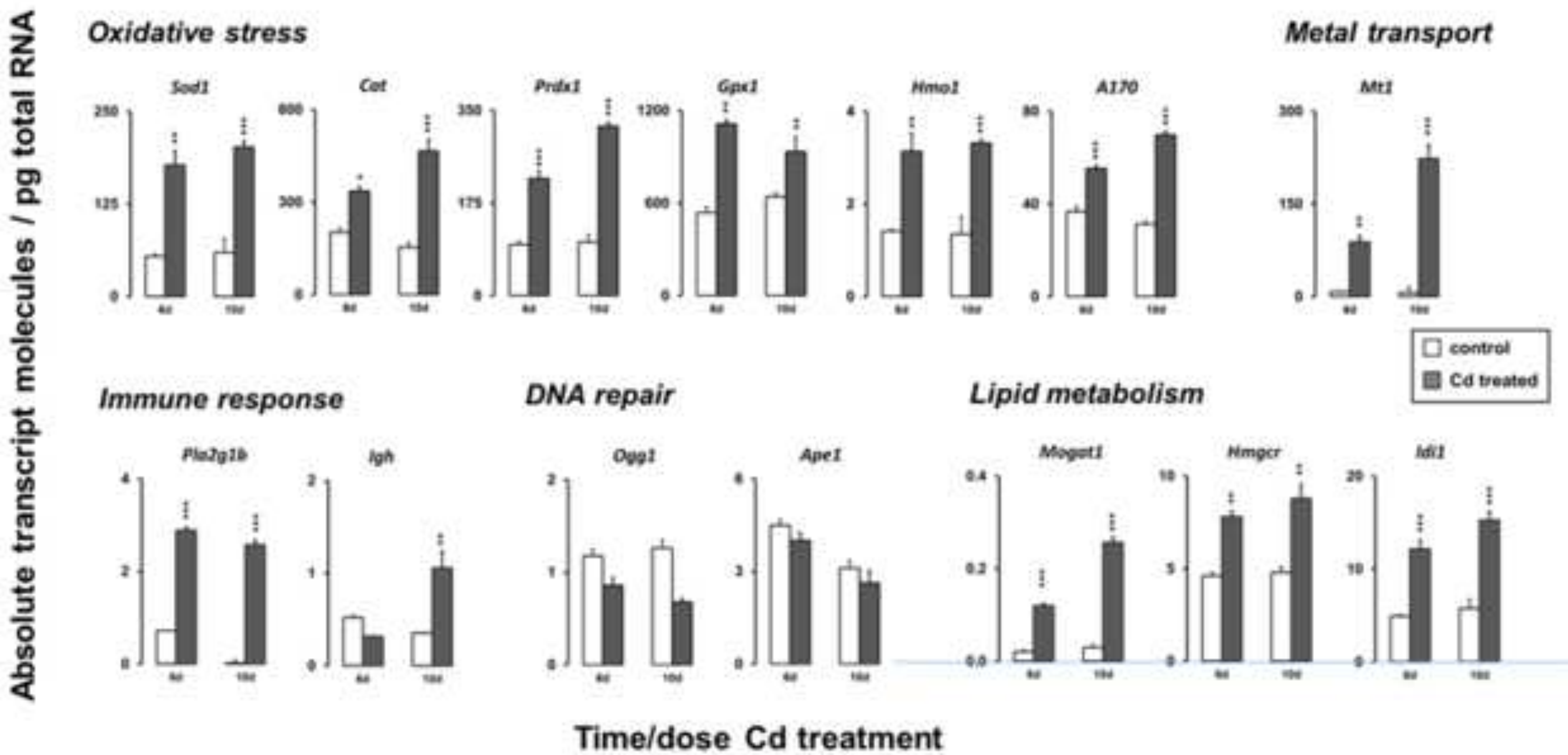

Figure 3
Click here to download high resolution image

Figure 3.

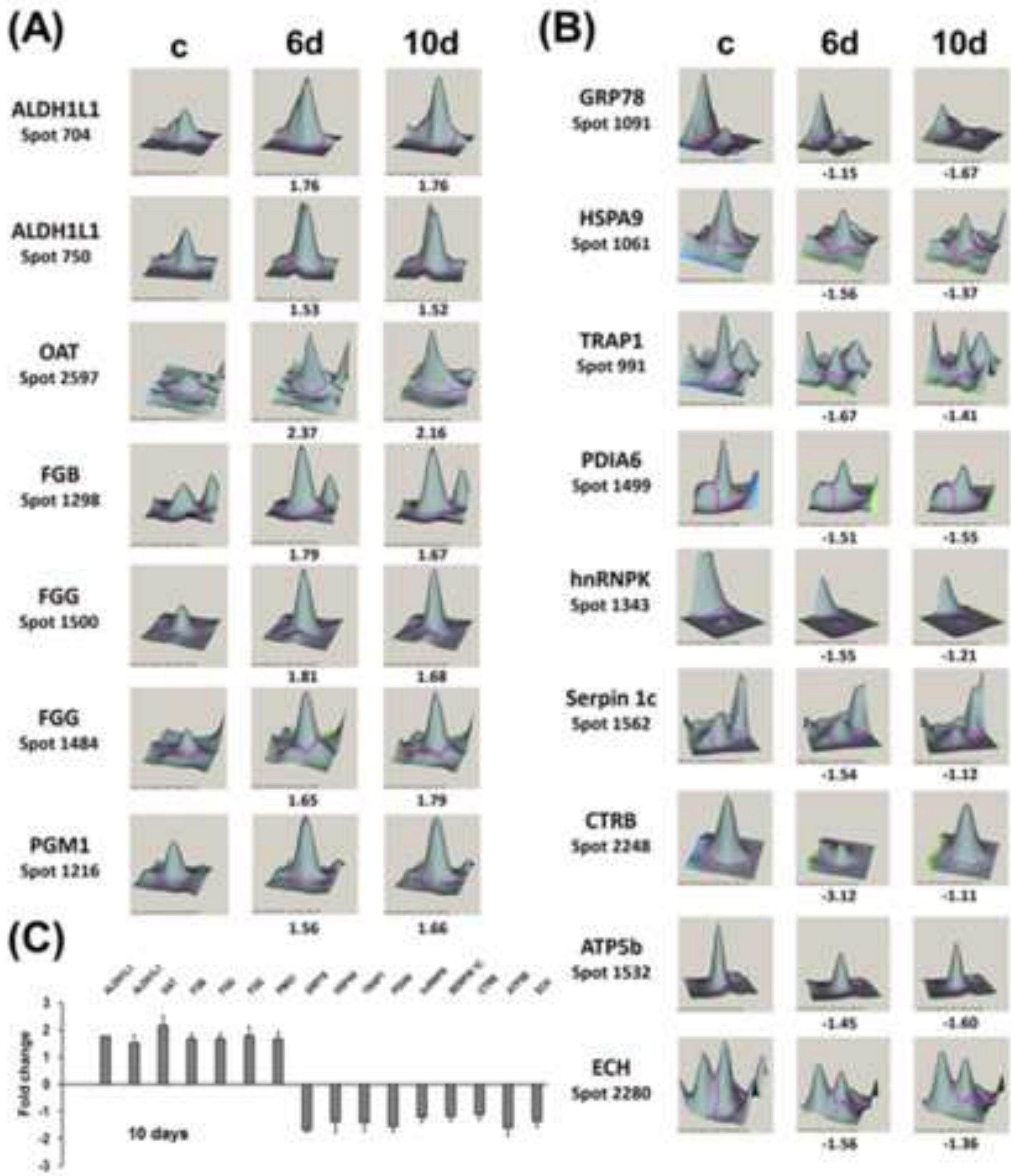

Figure 4
Click here to download high resolution image

Figure 4.

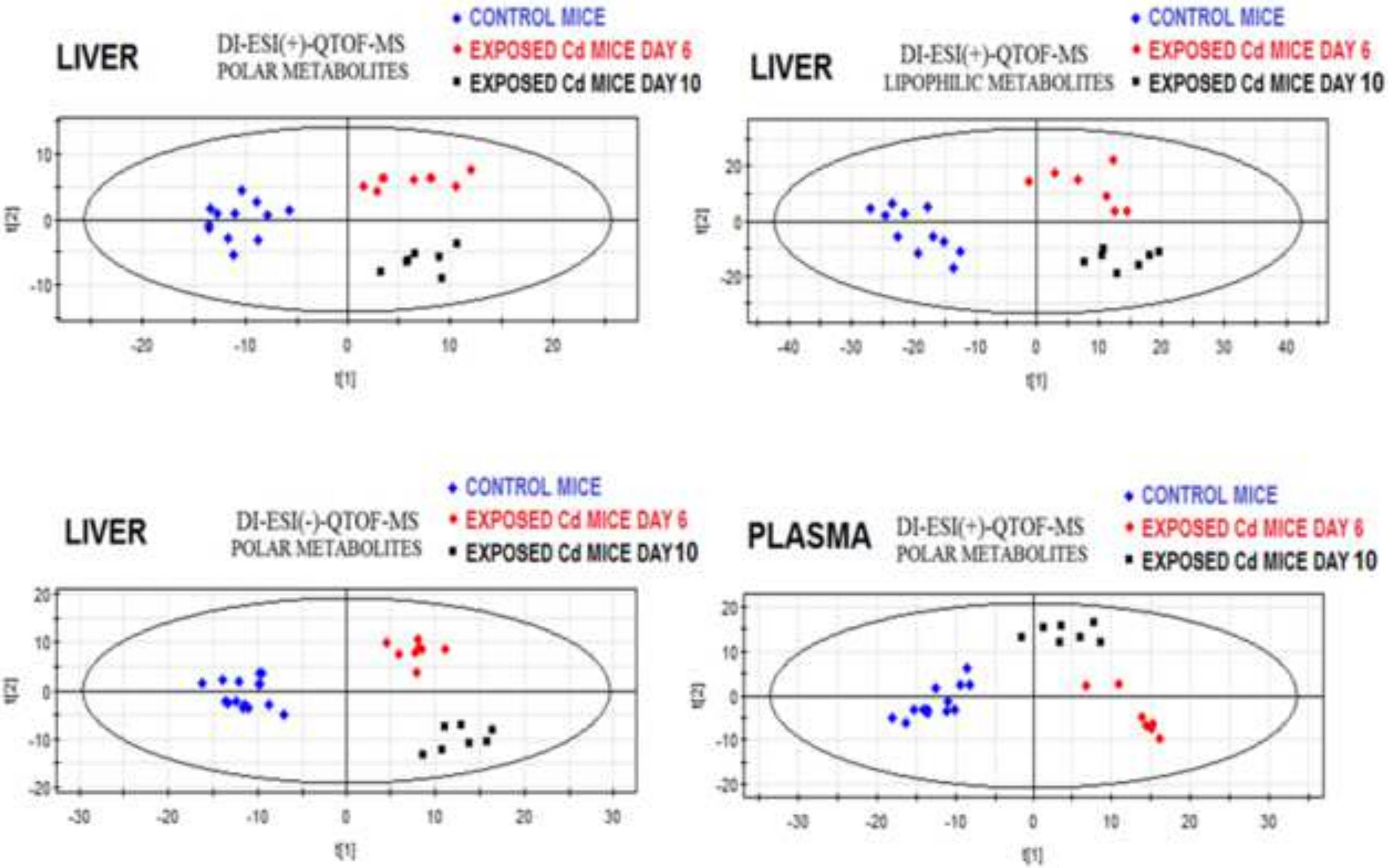

Figure 5
Click here to download high resolution image

Figure 5.

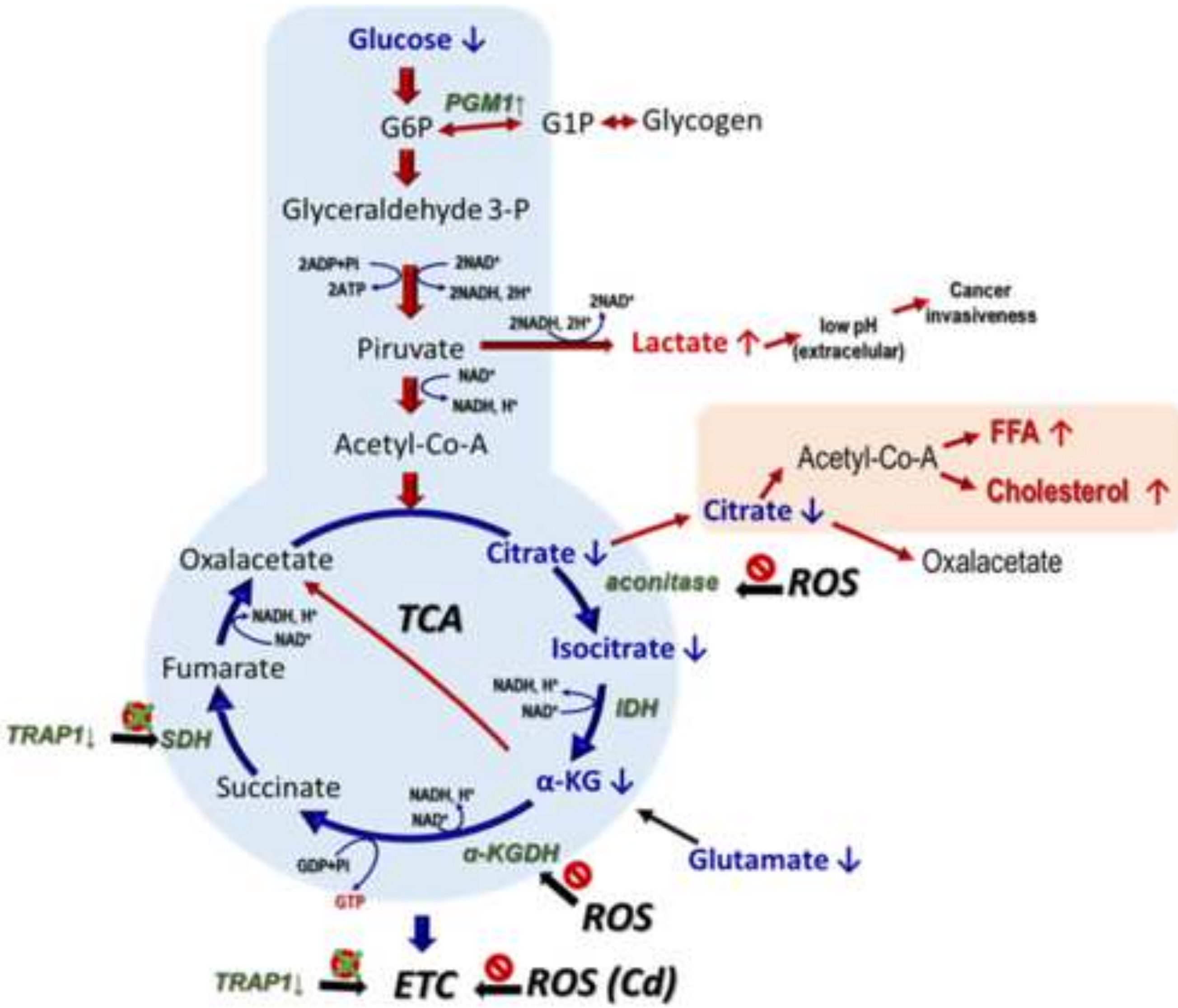

Table 1
Click here to download Table: Table 1.-DIGE identifies differ. Expressed proteins.docx

Table 1. Differentially expressed proteins in the liver of Cd treated *M. musculus* mice, identified by Mascot search based on MALDI-TOF–MS/MS data.

Master No[a]	Protein name[b] / Functional category	Symbol[b]	Uniprot ID[b]	Peptides mached	Sequence coverage (%)	Protein SCORE	Mass (kDa) Theor	Mass (kDa) Exp	PI Theor	PI Exp
	Stress response									
704	Aldehyde dehydrogenase family 1 member L1	ALDH1L1	Q8R0Y6	51	57	968	99.5	99.0	5.6	5.6
750	Aldehyde dehydrogenase family 1 member L1	ALDH1L1	Q8R0Y6	29	30	284	99.5	98.9	5.6	5.8
991	Heat shock protein 75 kDa mitochondrial	TRAP1	Q9CQN1	13	16	147	80.3	81.0	6.6	6.6
1061	Hspa9, Stress-70 protein	HSPA9	Q3TW93	26	35	500	73.8	73.7	5.91	5.5
1091	Hspa5, 78 kDa glucose-regulated protein	GRP78	P20029	26	36	387	72.5	72.5	5.1	5.0
1343	Heterogeneous nuclear ribonucleoprotein K	hnRNPK	P61979-2	17	33	151	51.3	55.5	5.7	5.5
1499	Protein disulfide-isomerase A6-like	PDIA6	Q922R8	16	29	324	47.6	52.7	6.3	5.3
2597	Ornithine aminotransferase, mitochondrial	OAT	P29758	7	20	123	50.6	23.0	5.0	6.2
	Immune response									
1298	Fibrinogen beta chain	FGB	Q8K0E8	21	35	384	55.4	56.8	6.8	6.1
1484	Fibrinogen gamma chain	FGG	Q3UER8	15	26	177	50.0	51.0	5.5	5.6
1500	Fibrinogen gamma chain	FGG	Q3UER8	17	33	251	50.0	52.0	5.5	5.5
1562	Serpin 1c Alpha-1-antitrypsin 1-3	Serpin 1c	Q00896	10	17	132	46.0	50.1	5.3	4.6
2248	Chymotrypsinogen B	CTRB	Q9CR35	10	38	98	28.4	29.9	4.9	5.0
	Energy homeostasis									
1216	Phosphoglucomutase-1	PMG1	Q9D0F9	33	49	357	61.8	60.9	6.3	6.4
1532	ATP synthase subunit beta, mitochondrial	ATP5B	P56480	28	46	624	56.3	51.6	5.2	4.9
2080	Δ(3,5)-Δ(2,4)-dienoyl-CoA isomerase, mitochondrial	ECH	O35459	16	42	216	36.4	35.8	7.6	6.2

[a]The numbering of the spots is arbitrary
[b]Protein name, symbol and identifier (ID) as UniProtKB/Swiss-Prot database.
[c] MOWSE protein score based on MS data.

Table 2. Biomarkers from liver and plasma of mice (*Mus musculus*) exposed to cadmium during 10 days.

Altered metabolites by DIMS				
Metabolites	***m/z***[a]	***Mode of acquisition***[b]	***Target Organ***	***Variation following Cd exposure***[c]
Choline	104.09 (H+)	ESI(+)	Liver and plasma	↑
Phosphocholine	185.10 (H+)	ESI(+)	Liver	↑
Lyso-phosphatidylcholines (Lyso-PC)	450-600	ESI(+)/ESI(-)	Liver	↑
Creatinine	114.05 (H+)	ESI(+)	Liver	↑
Capric acid (C10:0)	171.1 $(-H^+)$	ESI(-)	Liver	↑
Lauric acid (C12:0)	199.2 $(-H^+)$	ESI(-)	Liver	↑
Myristic acid (C14:0)	227.2 $(-H^+)$	ESI(-)	Liver	↑
Palmitic acid (C16:0)	255.2 $(-H^+)$	ESI(-)	Liver	↑
Palmitoleic acid (C16:1)	253.2 $(-H^+)$	ESI(-)	Liver	↑
Stearic acid (C18:0)	283.2 $(-H^+)$	ESI(-)	Liver	↑
Oleic acid (C18:1)	281.2 $(-H^+)$	ESI(-)	Liver	↑
Linoleic acid (C18:2)	279.2 $(-H^+)$	ESI(-)	Liver	↑
Linolenic acid (C18:3)	277.2 $(-H^+)$	ESI(-)	Liver	↑
Glutamine	147.08 (H^+)	ESI(+)	Liver	↑
Lactic acid	89.04 $(-H^+)$	ESI(-)	Liver and plasma	↑
Diglycerides	600-700	ESI(+)/ESI(-)	Liver	↑
Triglycerides	850-950	ESI(+)/ESI(-)	Liver	↑
Taurine	124.01 $(-H^+)$	ESI(+)	Liver and plasma	↓
Creatine	132.04 (H+)	ESI(+)	Liver	↓
Phenylalanine	169.07 (H+)	ESI(+)	Liver	↓
Glutamate	148.05 (H+)	ESI(+)	Liver and plasma	↓
	146.05 (-H+)	ESI (-)	Liver	
Citrate	193.03 (H^+)	ESI(+)	Liver and plasma	↓
Glucose	203.05 (Na^+)	ESI(+)	Plasma	↓
	215.03 (Cl^-)	ESI (-)		
Phosphatidylcholines (PC)	700-850	ESI(+)	Liver	↓

Altered metabolites concentration[d] ***in plasma by GC-MS*** **(nmol/l)**			
Metabolites	***Control mice***	***Cd exposed mice***[e] ***6***th ***day***	***Cd exposed mice***[e] ***10***th ***day***
Lactic acid	1.470 ± 0.100	1.630 ± 0.140	1.940 ± 0.210
Glutamine	0.568 ± 0.031	0.621 ± 0.026	0.672 ± 0.033
Cholesterol	1.460 ± 0.090	1.550 ± 0.120	1.680 ± 0.096
Phenylalanine	0.063 ± 0.003	0.062 ± 0.004	0.059 ± 0.005
Isocitric acid	0.521 ± 0.016	0.499 ± 0.034	0.478 ± 0.022
Citric acid	3.330 ± 0.410	3.140 ± 0.160	2.840 ± 0.180
Glucose	7.720 ± 0.510	7.410 ± 0.370	6.540 ± 0.690
α-Ketoglutarate	0.138 ± 0.011	0.121 ± 0.014	0.102 ± 0.011
Glutamic acid	0.141 ± 0.090	0.123 ± 0.011	0.104 ± 0.012
Isoleucine	0.072 ± 0.008	0.061 ± 0.009	0.048 ± 0.010

[a]The m/z ratios of the metabolites were measured to a precision of 0.01 Da.
[b]Metabolomic experiments of liver and plasma extracts from mice exposed to Cd were performed by DIMS in a mass spectrometer QSTAR XL Hybrid system (Applied Biosystems) using an electrospray ionization source (ESI). Both extracts were analyzed in positive (ESI+) and negative (ESI-) ion modes resulting different profiles in a wide spectral range (m/z 50-1100).
[c]Variations compared to control mice: ↑, increasing signal intensity;↓, decreasing signal intensity
[d]Data are mean ± SD of metabolite determination by by GC-MS in the plasma of five individual mice
[e]Statistical significant differences between the Cd treated animals and the controls at the $p<0.05$ level determined with Student's *t*-test are indicated In bold.

Supplementary Material 1
Click here to download Supplementary Material: Supp Inf Table 1.-Primers used in this work.docx

Supplementary Material 2

Click here to download Supplementary Material: Supp Inf Table 2. - Cd concentration in liver and plasma of experimental mice.docx

Supplementary Material 3
Click here to download Supplementary Material: Supp Inf Table 3. Variance in mouse gene expression.docx